Volume 2 Issue 4, December 2022

COMPLEX ENGINEERING SYSTEMS

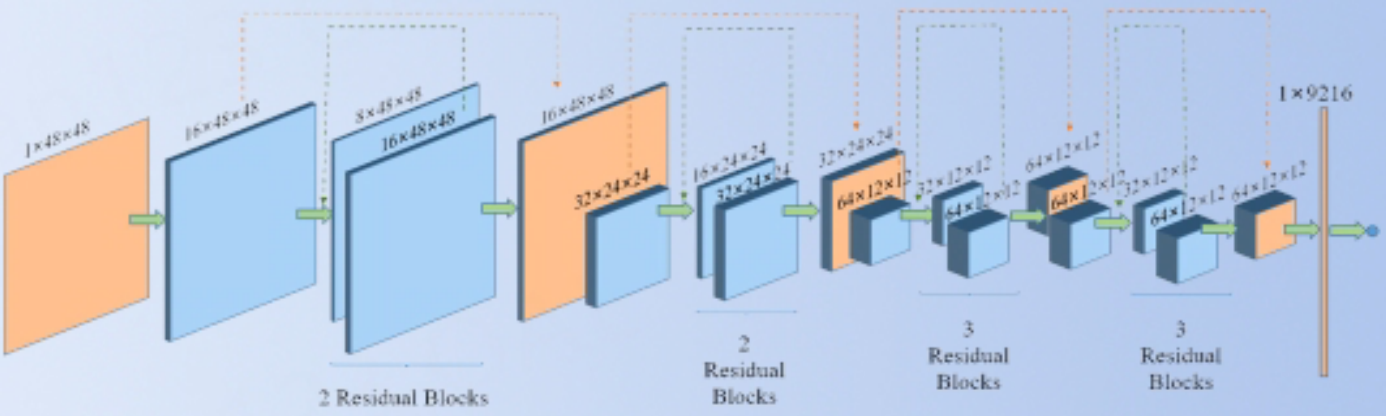

Pulsar identification based on generative adversarial network and residual network

Zelun Bao, Guiru Liu, Yefan Li, Yanxi Xie, Yang Xu, Zifeng Zhang, Qian Yin, Xin Zheng

Open Access
ISSN 2770-6249 (Online)
www.comengsys.com

EDITORIAL BOARD

GENERAL INFORMATION

About the Journal

Complex Engineering Systems (*CES*) are composed of a set of interconnected systems that their collective behaviors or properties are difficult to be predicted or managed. The context of *Complex Engineering Systems* (*CES*) is concerned with developing multi-component engineering systems, designs, or algorithms to exploit those unpredictable collective behaviors or properties. Complexity in engineering systems is in general manifested in component, product, system, interconnections of interacting subsystems or multidisciplinary system designs. In a broad sense, complexity is related to the expected amount of information may need to describe a dynamical system.

The primary objective of this journal is to provide a high-level platform for researchers and practitioners to disseminate theoretical- or engineering-oriented research output achievements within the context of *Complex Engineering Systems* (*CES*)that fosters knowledge sharing in different branches of engineering discipline. *Complex Engineering Systems* (*CES*) also publishes novel theoretical methods, algorithms, simulations, experiments, and case studies as applications of state-of-the-art research in *Complex Engineering Systems* (*CES*).

Information for Authors

Manuscripts should be prepared in accordance with Author Instructions.
Please check https://comengsys.com/pages/view/author_instructions for details.
All manuscripts should be submitted online at https://oaemesas.com/login?JournalId=comengsys.

Copyright

Permissions

Disclaimer

Publisher

OAE Publishing Inc.
245 E Main Street Ste 107, Alhambra CA 91801, USA
Website: www.oaepublish.com

Contacts

E-mail: editorial@comengsys.com
Website: https://comengsys.com/

Complex Engineering Systems

CONTENTS

Volume 2 / Issue 4 /

Research Article

Sathyan *et al*. *Complex Eng Syst* 2022;2:18
DOI: 10.20517/ces.2022.41

Complex Engineering Systems

Research Article

Open Access

Interpretable AI for bio-medical applications

Anoop Sathyan[1], Abraham Itzhak Weinberg[2], Kelly Cohen[1]

[1]Department of Aerospace Engineering, University of Cincinnati, Cincinnati, OH 45231, USA.
[2]Department of Management, Bar-Ilan University, Ramat Gan 5290002, Israel.

Correspondence to: Dr. Anoop Sathyan, Department of Aerospace Engineering, University of Cincinnati, Cincinnati, OH 45231, USA. E-mail: sathyaap@ucmail.uc.edu; ORCID: 0000-0003-2414-9515

How to cite this article: Sathyan A, Weinberg AI, Cohen K. Interpretable AI for bio-medical applications. *Complex Eng Syst* 2022;2:18. http://dx.doi.org/10.20517/ces.2022.41

Received: 11 Oct 2022 **First Decision:** 24 Nov 2022 **Revised:** 9 Dec 2022 **Accepted:** 19 Dec 2022 **Published:** 28 Dec 2022

Academic Editor: Hamid Reza Karimi **Copy Editor:** Fanglin Lan **Production Editor:** Fanglin Lan

Abstract

This paper presents the use of two popular explainability tools called Local Interpretable Model-Agnostic Explanations (LIME) and Shapley Additive exPlanations (SHAP) to explain the predictions made by a trained deep neural network. The deep neural network used in this work is trained on the UCI Breast Cancer Wisconsin dataset. The neural network is used to classify the masses found in patients as benign or malignant based on 30 features that describe the mass. LIME and SHAP are then used to explain the individual predictions made by the trained neural network model. The explanations provide further insights into the relationship between the input features and the predictions. SHAP methodology additionally provides a more holistic view of the effect of the inputs on the output predictions. The results also present the commonalities between the insights gained using LIME and SHAP. Although this paper focuses on the use of deep neural networks trained on UCI Breast Cancer Wisconsin dataset, the methodology can be applied to other neural networks and architectures trained on other applications. The deep neural network trained in this work provides a high level of accuracy. Analyzing the model using LIME and SHAP adds the much desired benefit of providing explanations for the recommendations made by the trained model.

Keywords: Explainable AI, LIME, SHAP, neural networks

1. INTRODUCTION

In recent years, we have witnessed growth in the usage and implementation of machine learning based decision making and predictive analytics. Practically speaking, machine learning models are ubiquitous [1]. One of the reasons for this growth is the contribution of machine learning to their users and decision makers. In recent times, there has been a rise in the development of new computational infrastructures such as cloud storage and parallel computation [2], which has contributed to faster training of the models. Many papers contribute to the effort of developing machine learning models that excel in metrics such as accuracy, efficiency and running time. The more complex models are usually more accurate [3,4]. However, the ability of humans to understand it is negatively correlated to model complexity [5]. One of the challenges to eXplainable AI (XAI) is its implementation in real-life applications. XAI has inherent challenges such as lack of expertise, inherently biased choices, lack of resiliency for data changes, algorithms and problems interference challenges, local context dependency of the explanations and lack of causality of explanations between input and output [6]. These challenges intensify for clinical and medical real-life use cases such as in the breast cancer use case we consider in this work. In order to overcome these challenges, there is a need for a strong interaction between the XAI system and the decision makers. In our case, the domain experts, radiologists and physicians need to examine the XAI results and add their own perspectives based on their prior knowledge before making final decisions. In addition, they can add their feedback in order to improve and fine-tune the XAI system. Another way to increase the trustworthiness of the XAI can be synergy between different XAI approaches and algorithms. In our case, we use Local Interpretable Model-Agnostic Explanations (LIME) and Shapley Additive exPlanations (SHAP). Each of them has a different approach to extract the explanations of the model predictions. When both XAI approaches provide the same or similar results, it is an indication that the user can have higher confidence in the interpretability of the model.

To realize the immense economic and functional potential in AI applications that have stringent safety and mission critical requirements in areas such as healthcare, transportation, aerospace, cybersecurity, and manufacturing, existing vulnerabilities need to be clearly identified and addressed. The end user of such applications as well as the taxpaying public will need assurances that the fielded systems can be trusted to deliver as asked. Moreover, recent developments evaluating the trustworthiness of high-performing "black-box" AI have classified them using the term "Brittle AI", as a retrospective look at DARPA's explainable AI program. These developments coupled with a growing belief in the need for "Explainable AI" have led major policy makers in the US and Europe to underscore the importance of "Responsible AI".

Recently, on June 28, 2022, a group of Cruise robotaxis abruptly stopped working on a street in San Francisco, California, which caused traffic to stop for several hours until employees of the company arrived. Cruise, which is backed by General Motors and Honda, has been testing its technology in San Francisco since February, but only launched a commercial robotaxi service a week prior to this malfunction. The cars have no human driver at all but operate under certain restrictions (good weather and a speed limit of 30mph). They only offer the taxi service in a dedicated area of the city during after-hours between 10PM and 6AM [7]. While no one was hurt in this instance, several questions are raised concerning the maturity of the autonomous system technology and the need to ensure that these autonomous systems operate as intended. The outcome is that the public is concerned and does not trust such systems. In order to handle such events in future, we can find several approaches in literature. Some of the methods include observer fault estimation based on sensors [8], nature optimal control systems [9] and predictive control models [10]. All the approaches add a layer to the system that is supposed to detect any faulty behavior of the system. The mission in such cases is to translate the predictions of the control systems into a way that its operators and decision makers will be able to understand. The system has to provide a way to explain what happened and what action has to be taken by humans. This is one of the deliverables that XAI is supposed to yield.

According to the National Institute of Standards and Technology (NIST) [11], determining that an AI system is

trustworthy just because all system requirements have been addressed is not enough to guarantee widespread adoption of AI. Moreover, according to NIST, "It is the user, the human affected by the AI, who ultimately places their trust in the system," and furthermore, "alongside research toward building trustworthy systems, understanding user trust in AI will be necessary to minimize the risks of this new technology and realize its benefits.

In June 2022, Kathleen Hicks, Deputy Secretary of Defense, released a report that clarifies the DoD perspective concerning trust in AI systems as follows: "The Department's desired end state for Responsible AI (RAI) is trust. Trust in DoD AI will allow the Department to modernize its warfighting capability across a range of combat and non-combat applications, considering the needs of those internal and external to the DoD. Without trust, warfighters and leaders will not employ Al effectively and the American people will not support the continued use and adoption of such technology"[12]. This paradigm shift in policy will have a major impact on the continued development and fielding of AI systems for DoD and for the safety critical systems in the civilian arenas such as health, energy transportation etc.

In line with DoD's perspectives on trust in AI, it is important that users of AI models be able to assess the model, its decisions and predictions by their ability to understand it. In addition, for better understanding, the users would like to get answers to questions such as what needs to be done to change the model or its prediction. This is one of the motivations for the rapid growth in popularity of the paradigm called XAI. The interaction between machine learning models and their users has become one of the crucial points in usage and implementation of AI systems. Many emerging algorithms try to solve this human-machine interaction by providing a meaningful explanation for the model.

There are ways to classify the XAI approaches by several criteria[13] such as: model dependency, sample particularity, explainability timing and the interaction between the explanation to the model itself. More specifically, independence of the explainability of the model itself is called model agnostics. The explanation of the entire model is called global explainability, while explaining a particular sample is called local explainability. The position of the explainability process in model life cycle determines whether the explainability is pre-model, in-model or post-model.

This paper uses two popular approaches for XAI: LIME[14,15] and SHAP[16]. Both are attribution-based explanation models. Attribution-based explanation models find and quantify the most contributed features on model predictions. In addition, both models are relatively easy to use, and their results can be plotted and easily interpreted. LIME and SHAP in our case are used as Post-hoc models, locally interpretable and model agnostic. Although both LIME and SHAP explain the predictions made by the trained model, they use different approaches. SHAP relies on Shapley values for finding the best contributing features[16], while LIME explains the model decision in a local region around a particular sample[14]. Each approach has its own benefits. Using both approaches supports the explainability level of our deep learning model. Using both LIME and SHAP allows us to compare the insights gained using the two tools. Additionally, since the two tools work independently of each other, the commonalities between the insights gained can be used to gain a better understanding of the trained model as well as how the different features play a role in the diagnosis/prediction.

2. XAI FOR HEALTHCARE

The implementation of XAI for increasing trustworthiness can also be found in biomedical studies such as drug-drug interactions prediction[17] as well as classification of protein complexes from sequence information[18]. In our case, we use the XAI for the interpretability of breast cancer predictions. The combination of the two has a fast-growing demand[2]. The benefits of implementing XAI in medical fields provide opportunity for prevention and better treatment[2]. The XAI helps clinicians in the diagnostic process as well as their

recommendations[2]. This in turn helps the patients to trust the model results and system recommendations. This can also increase the probability that the patient will accept and follow the recommended medical treatment. Moreover, XAI can decrease the probability of error in the diagnostic process since it helps clinicians to focus on the relevant data and help them to better understand the model recommendations.

XAI is an evolving field. As mentioned before, at this current stage, even state-of-the-art XAI algorithms have disadvantages. In literature, we can find approaches that aim to improve some aspects. One of the main challenges of using XAI in healthcare environments is the need to remain neutral regarding preferences. We can find a bona fide approach called scientific explanation in AI (sXAI) that can be used in the field of medicine and healthcare[19]. An additional approach based on integrated Electronic Medical Records (EMR) medical systems is described in[20]. The approach focuses on explainability and interoperability from the human aspect. Ensemble of machine learning (ML) can also increase the level of interpretability, as can be seen in[21]. In[21], the author use ensemble of ML for logic driving of anthropometric measurements influencing body mass index (BMI). Additional evidence for the implementations of several XAI models is mentioned in[22]. The paper shows how integrating XAI models helps to increase the persuasive and coherence levels in the decision making of clinicians and medical professionals teams. The usage of XAI has shown an improvement in transparency and reliability in the field of neuroscience field[23].

In this paper, we apply some XAI concepts to a use case applicable to the medical field. Our work focus on XAI implementation for breast cancer diagnostics. Our research uses the commonly researched UCI breast cancer dataset. We focus on breast cancer since it is the most common type of cancer amongst women[24]. The usage of XAI for diagnostics and prediction of breast cancer can impact and help a large number of patients. The UCI breast cancer dataset includes 569 data points[25]. Each data point consists of 32 attributes that include the ID number, the diagnosis, and 30 features used as predictors in this work. The 30 predictors include the mean, standard deviation and the mean of 3 largest values of 10 features: (1) radius (mean of distances from center to points on the perimeter); (2) texture (standard deviation of gray-scale values); (3) perimeter; (4) area; (5) smoothness; (6) compactness; (7) concavity; (8) concave points; (9) symmetry; and (10) fractal dimension.

3. METHODOLOGY

3.1. LIME

LIME is one of the methodologies that is used to explain the predictions made by machine learning classifier models[26]. It can explain individual predictions made by text classifiers as well as classifiers that are modeled on tabular data.

In this work, we are focusing on using LIME to explain decisions made by a neural network classifier that works on tabular dataset. The process of LIME to explain individual predictions are as follows:

1. For each instance that needs to be explained, LIME perturbs the observation n times.
2. For tabular data, the statistics for each variable in the data are evaluated.
3. The permutations are then sampled from the variable distributions within the neighborhood of the original data point for which an explanation is being sought.
4. In our case, the original model is a neural network. The trained neural network model is used to predict the outcome of all permuted observations.
5. Calculate the distance from the perturbed points to the original observation and then convert it to a similarity score.
6. Select m features best describing the original model outcome for the perturbed data.
7. Fit a simple model (linear model) on the perturbed data, explaining the original model outcome with the m features from the permuted data weighted by its similarity to the original observation.
8. Extract the feature weights from the simple model and use these as explanations.

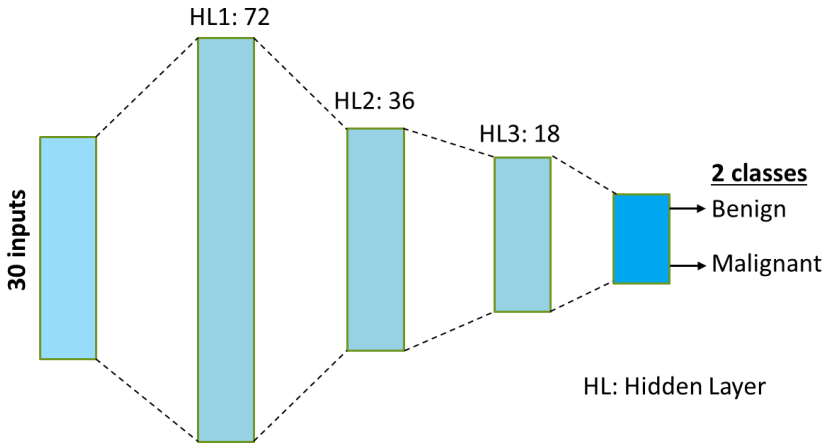

Figure 1. Schematic of the DNN used for classification into benign and malignant. The network uses 30 features and has three hidden layers (HL).

3.2. SHAP

SHAP is another methodology used for obtaining explanations for individual predictions. Additionally, SHAP can provide additional insights into predictions made across a set of data points. SHAP is based on Shapely values, a concept that is derived from game theory[16]. This is a game theoretic approach to explain any predictions made by a machine learning model. Game theory deals with how different players affect the overall outcome of a game. For the explainability of a machine learning model, SHAP considers the outcome from the trained model as the game and the input features that are used by the model as the players. Shapley values are a way of representing the contribution of each player (feature) to the game (prediction).

Shapley values are based on the concept that each possible combination of features has an effect on the overall prediction made by the model. The SHAP process for explaining predictions is as follows[27]:

1. For a set of p features, there are 2^p possible combination of features. For example, a dataset that consists of three input features (x_1, x_2, x_3) will have the eight possible combinations: (a) no features, (b) x_1 (c) x_2, (d) x_3, (e) (x_1, x_2), (f) (x_2, x_3), (g) (x_1, x_3), (h) (x_1, x_2, x_3).
2. Models are trained for each of the 2^p combinations. Note that the model that uses no features just outputs the mean of all output values in the training data. This is considered as the baseline prediction (y_ϕ).
3. For the data point whose output needs to be explained, the remaining $2^p - 1$ models are evaluated.
4. Marginal contribution of each of the models. Marginal contribution of model-j is calculated using the difference between the predictions made by model-j and the baseline prediction.

$$MC_j = \tilde{y}_j - y_\phi \tag{1}$$

5. To obtain the overall effect of a feature on the prediction, the weighted mean of the marginal contributions of every model containing that feature is evaluated. This is called the Shapley value of the feature for the particular data point.

3.3. Deep neural network

We use a deep neural network (DNN) to diagnose a patient into two classes: benign or malignant. The architecture of the DNN is shown in Figure 1. It uses the 30 features mentioned before to make predictions. The development and training of the DNN was done in PyTorch[28]. Rectified linear units (ReLU) are used as the activation functions in the hidden layers, and softmax activation is used at the output layer to output the probabilities to the two output classes.

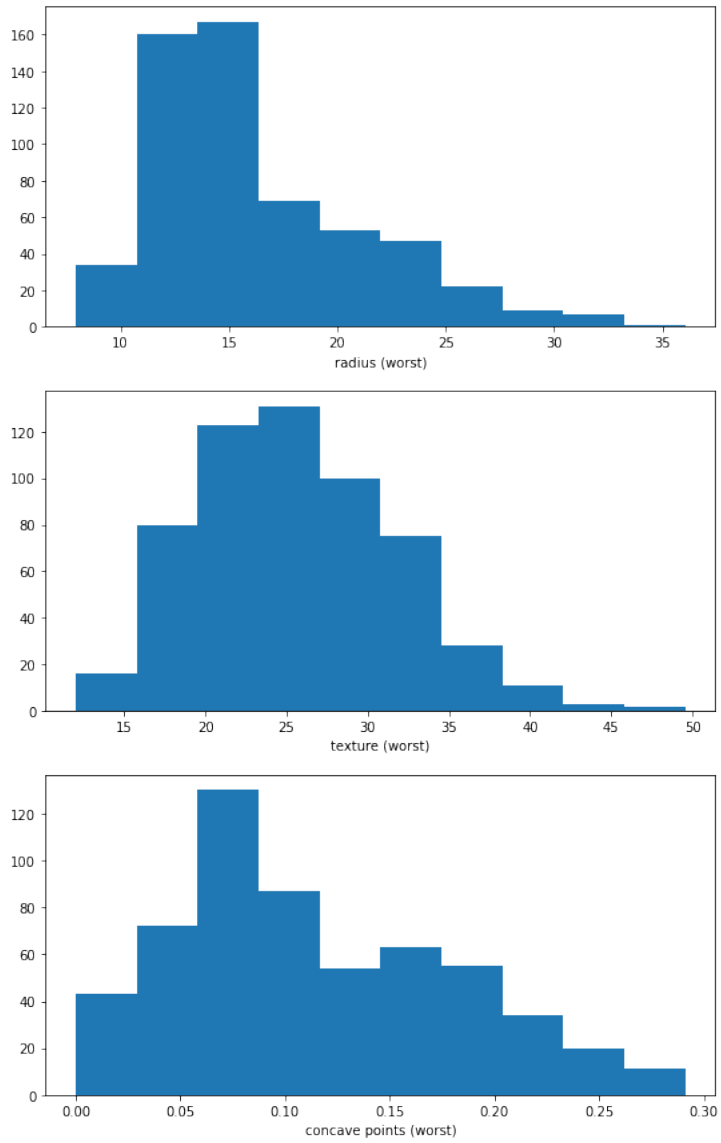

Figure 2. Histograms for three of the important features: radius (worst), texture (worst) and concave points (worst)

4. RESULTS & DISCUSSION

The UCI Breast Cancer Wisconsin dataset used an 80%-20% split. This means 80% of the data were randomly chosen for training and the remaining 20% was used for testing. To highlight the data distribution, histograms are shown for three of the important input features in Figure 2.

Since this is a classification problem, cross entropy was used as the loss function. Adam optimizer was used with a learning rate of 0.001 for training the DNN. A batch size of 32 was used when modifying the parameters during the optimization. The DNN was trained on 100 epochs and the trained DNN provided an accuracy of 97% on the test data. This is on the higher end of performance among models trained on this dataset, with the best accuracy noted for this dataset to be 98.6%[29]. It is to be noted that this work is not focused on the performance of DNN in terms of accuracy, but instead on explaining the decisions or predictions made by the trained DNN. The trained DNN is further analyzed using LIME and SHAP to understand and explain its predictions.

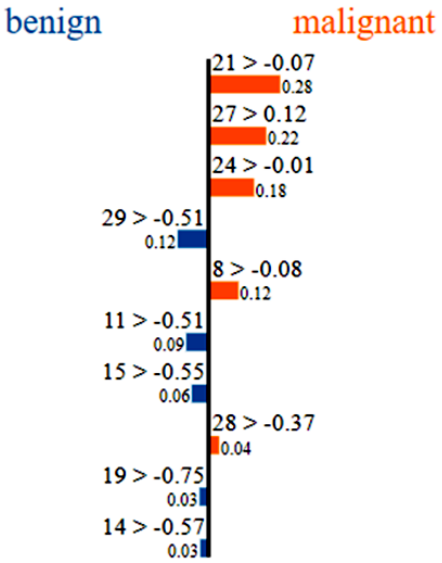

Figure 3. LIME output for a data point that is classified as malignant.

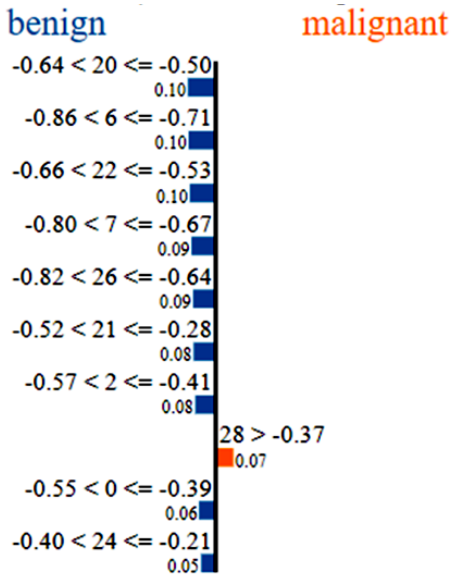

Figure 4. LIME output for a data point which is classified as benign.

4.1. Results with LIME

LIME is used to explain the predictions made by the DNN on the patients (data points) identified in the test set. The outputs from LIME are shown for two data points from the test set in Figures 3 and 4. The first number above each horizontal bar refers to the index of the input variable. The length of each bar is proportional to the contribution factor of that input variable mentioned next to it. For the data point in Figure 3, inputs 21, 27 and 24 are the three most contributing variables that drive the prediction to malignant with contribution factors of 0.28, 0.22 and 0.18, respectively. There are some variables such as inputs 29, 11, 15, etc. that try to drive the prediction to benign. However, the contributions of these inputs are lower for this particular data point.

For the data point in Figure 4, most of the major input contributions seem to drive the prediction correctly to

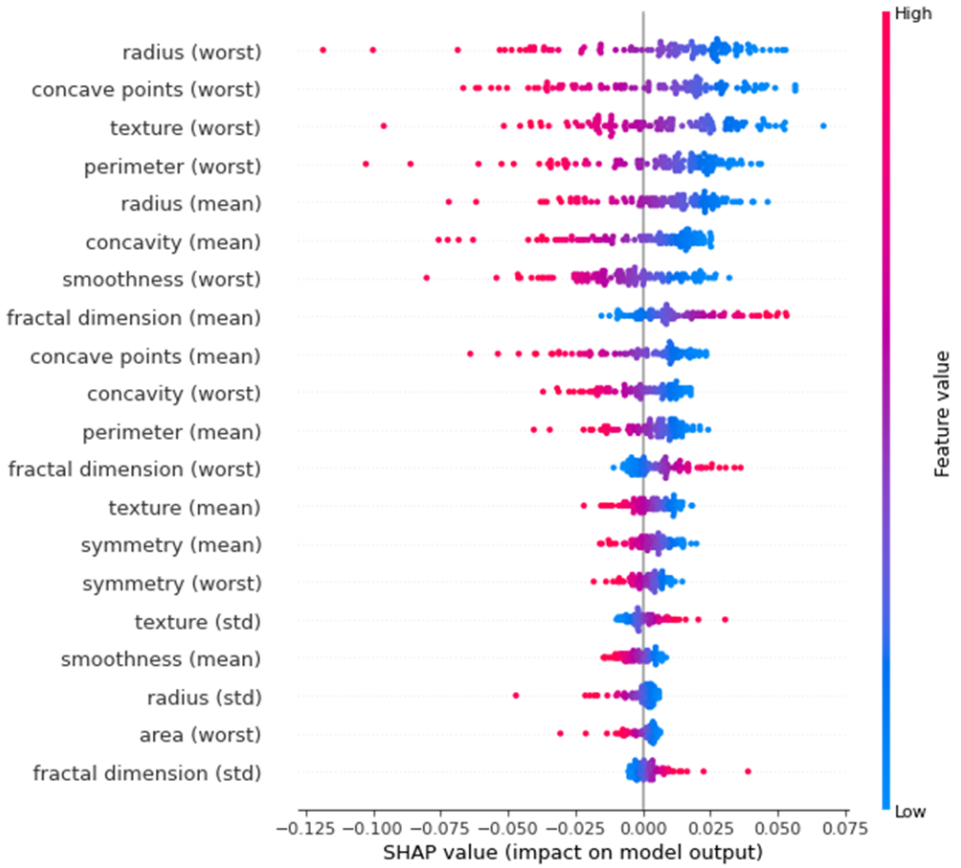

Figure 5. SHAP summary plot on the test data for the benign output class

benign. In this case, inputs 20, 6 and 22 (radius (worst), concavity (mean) and perimeter (worst), respectively) are the most important inputs, each with a contribution factor of 0.1. For these two cases, it is understood that lower values for most of the features indicate benign masses while higher values indicate malignancy. This is consistent with expert understanding of malignant masses [30]. The LIME outputs thus help us gain an understanding of the variables and their values that affect the predictions made by the trained DNN.

4.2. Results with SHAP

SHAP was also used to analyze the predictions made by the trained DNN on the data points from the test set. The Shapley values of each input feature can be evaluated for each data point. The mean of the absolute shapley values of each feature across the data can be used to evaluate the importance of the features. Figure 5 shows the summary plot of shapley values across the test data. The shapley values are plotted for the benign output class. Hence, higher shapley values imply higher chances of a benign prediction. The color of the points represents the feature values, with lower values shown by blue and higher values shown by red points. Overlapping points are jittered vertically. The input features are ordered in descending order of importance which is measured using the mean of the absolute shapley values across the data for feature. This can also be noticed from the fact that moving down, the distribution of shapley decreases.

From Figure 5, we can infer that lower values of certain features such as radius (worst), concave points (worst), texture (worst), etc. indicate a benign prediction. On the other hand, higher values for the same features indicate a malignant prediction. This is in line with expert's understanding of malignancy of breast masses as described in the UCI breast cancer Wisconsin database [30]. In fact, the features in this dataset are defined such that higher values indicate malignancy. Additionally, the SHAP summary plot also correctly identifies that the

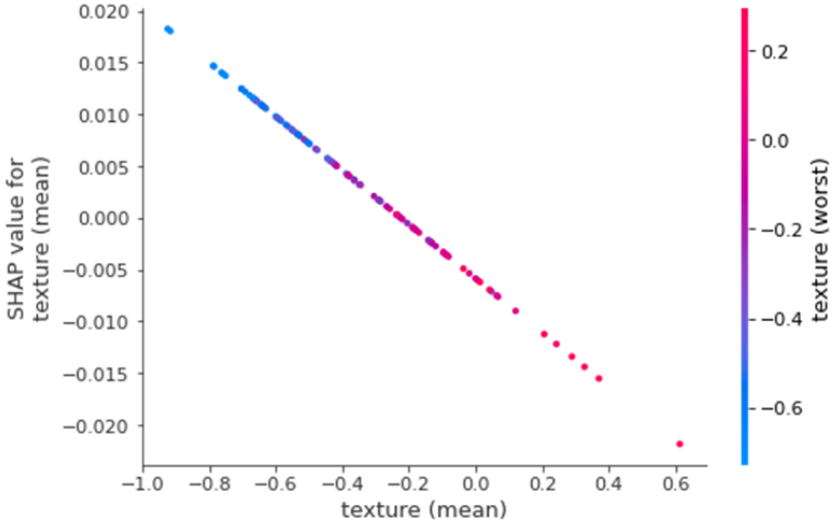

Figure 6. SHAP dependency plot for texture (mean). SHAP: Shapley Additive exPlanations.

worst values of the different variables are more important for differentiating between benign and malignant masses.

SHAP dependency plots can provide additional insights about the dependency between features and their effect on the shapley values. For example, Figure 6 shows the SHAP dependency plot for the input feature texture (mean). This feature has the highest dependency on another input feature texture (worst) and hence is also shown in the plot. It can be noticed that shapley values for texture mean linearly decreases with increasing texture (mean). Additionally, based on the colored points, it can be seen that higher texture (mean) also has higher texture (worst).

As another example, Figure 7 shows the SHAP dependency plot for the feature concave points (mean). The feature with the highest dependency on this feature is symmetry (std). Again, it can be seen that the shapley values for concave points (mean) linearly decrease with increasing values for the feature concave points (mean). However, symmetry (std) does not necessarily have a linear relationship with the chosen feature, as can be seen from the distribution in the colors of the different points on the plot. We can see points with low and high values of symmetry (std) for lower values of concave points (mean).

Certain commonalities can be found between the SHAP summary plot in Figure 5 and the LIME plots for individual data points from Figures 3 and 4. For example, Figure 3 shows that higher values of texture (worst), smoothness (worst) and concave points (worst) (inputs 21, 24 and 27, respectively) drive that data point to malignant prediction. The same can be noticed from the SHAP summary plot. Similarly, from Figure 4, lower values of radius (worst), concavity (mean) and perimeter (worst) (inputs 20, 6 and 22, respectively) drive that data point towards benign prediction. The same trend can be seen from the SHAP summary plot in Figure 5.

The above analysis suggests that explainability tools such as LIME and SHAP can be invaluable tools in analyzing trained models and understanding their predictions. These tools can help us obtain trends in the predictions from the trained models to explain the decisions made by the model. LIME and SHAP could be used for multi-class classification (with more than two classes)[31], regression[32] and other types of applications such as image processing using CNNs[33], etc. Since both tools have to run the trained model several times to produce explanations, it may not be useful for real-time explanations. The computational complexity of methods would depend on the computational time needed to make inferences. For example, larger neural

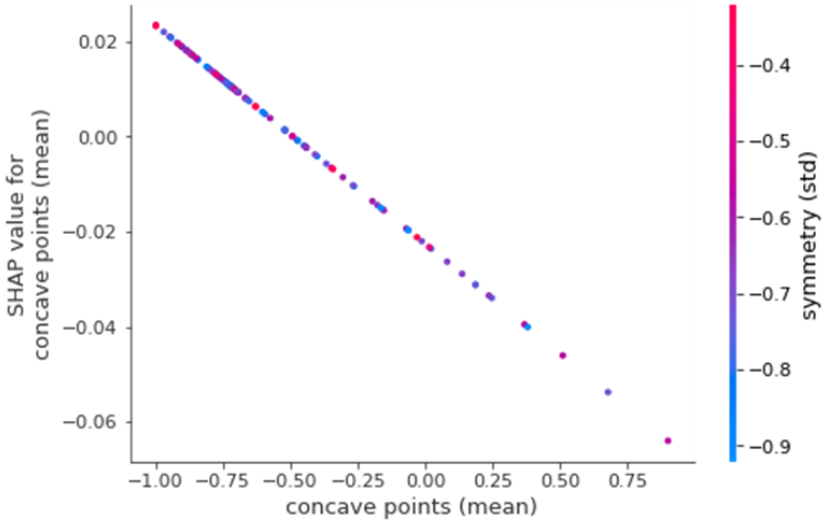

Figure 7. SHAP dependency plot for concave points (mean). SHAP: Shapley Additive exPlanations.

networks could be more complicated to use as inputs to LIME and SHAP. However, they can still be a valuable tool for obtaining explanations for applications that do not require real-time explanations or those that only require explanations during certain instances.

5. CONCLUSIONS AND FUTURE WORK

In this paper, we presented the use of two explainability tools, namely LIME and SHAP, to explain the decisions made by a trained DNN model. We used the popular Breast Cancer Wisconsin dataset from the UCI repository as the use case for our work. We presented the trends obtained using LIME and SHAP on the predictions made by the trained models. The LIME outputs were shown for individual data points from the test data. On the other hand, SHAP was used to present a summary plot that showed a holistic view of the effect of the different features on the model predictions across the entire test dataset. Additionally, the paper also presented common trends between the analysis results from both LIME and SHAP.

For future work, we plan to use these tools for other datasets, especially those with more than two output classes. It will be interesting to see how the results from LIME and SHAP analysis can help gain insights into datasets with a larger number of classes. The results from this paper are very encouraging to the research efforts on advancing explainability to deep learning based machine learning models. We also plan to make use of the abstract features derived within the DNN as possible input to LIME and SHAP. This may also help to understand the relevance of abstract features and may be useful for other aspects of machine learning, such as transfer learning.

5.1. Note

The Python code is available at this GitHub repository: https://github.com/sathyaa3p/xaiBreastCancer

DECLARATIONS

Authors' contributions

Made substantial contributions to conception and design of the study: Sathyan A, Weinberg AI, Cohen K
Training the models and interpretation of results: Sathyan A, Weinberg AI

Availability of data and materials

Not applicable.

Financial support and sponsorship

Research reported in this paper was supported by National Institute of Mental Health of the National Institutes of Health under award number R01MH125867.

Conflicts of interest

All authors declared that there are no conflicts of interest.

Ethical approval and consent to participate

Not applicable.

Consent for publication

Not applicable.

REFERENCES

1. Došilović FK, Brčić M, Hlupić N. Explainable artificial intelligence: a survey. In: 2018 41st International convention on information and communication technology, electronics and microelectronics (MIPRO). IEEE; 2018. pp. 0210–15. DOI
2. Markus AF, Kors JA, Rijnbeek PR. The role of explainability in creating trustworthy artificial intelligence for health care: a comprehensive survey of the terminology, design choices, and evaluation strategies. *J Biomed Inform* 2021;113:103655. DOI
3. Ribeiro MT, Singh S, Guestrin C. Model-agnostic interpretability of machine learning. arXiv preprint arXiv:160605386 2016.
4. Gilad-Bachrach R, Navot A, Tishby N. An information theoretic tradeoff between complexity and accuracy. In: Learning Theory and Kernel Machines. Springer; 2003. pp. 595–609.
5. Linardatos P, Papastefanopoulos V, Kotsiantis S. Explainable AI: a review of machine learning interpretability methods. *Entropy* 2020;23:18. DOI
6. de Bruijn H, Warnier M, Janssen M. The perils and pitfalls of explainable AI: Strategies for explaining algorithmic decision-making. *Government Information Quarterly* 2022;39:101666. DOI
7. Khalid A. A swarm of Cruise robotaxis blocked San Francisco traffic for hours; 2022. Available from: https://www.engadget.com/cruise-driverless-taxis-blocked-san-francisco-traffic-for-hours-robotaxi-gm-204000451.html. [Last accessed on 22 Dec 2022]
8. Djordjević V, Stojanović V, Pršić D, Dubonjić L, Morato MM. Observer-based fault estimation in steer-by-wire vehicle. *Eng Today* 2022;1:7–17. DOI
9. Pršić D, Nedić N, Stojanović V. A nature inspired optimal control of pneumatic-driven parallel robot platform. *Proceedings of the Institution of Mechanical Engineers, Part C: Journal of Mechanical Engineering Science* 2017;231:59–71. DOI
10. Morato MM, Bernardi E, Stojanovic V. A qLPV nonlinear model predictive control with moving horizon Estimation. *Complex Eng Syst* 2021;1:5. DOI
11. Stanton B, Jensen T. Trust and artificial intelligence. preprint 2021. Available from: https://tsapps.nist.gov/publication/get_pdf.cfm?pub_id=931087 [Last accessed on 22 Dec 2022]
12. U.S. department of defense responsible artificial Intelligence strategy and implementation pathway. Department of Defense; 2022. Available from: https://media.defense.gov/2022/Jun/22/2003022604/-1/-1/0/Department-of-Defense-Responsible-Artificial-Intelligence-Strategy-and-Implementation-Pathway.PDF [Last accessed on 22 Dec 2022]
13. Singh A, Sengupta S, Lakshminarayanan V. Explainable deep learning models in medical image analysis. *J Imaging* 2020;6:52. DOI
14. Ribeiro MT, Singh S, Guestrin C. " Why should i trust you?" Explaining the predictions of any classifier. In: Proceedings of the 22nd ACM SIGKDD International Conference on Knowledge Discovery and Data Mining; 2016. pp. 1135–44.
15. Dieber J, Kirrane S. Why model why? Assessing the strengths and limitations of LIME. arXiv preprint arXiv:201200093 2020. DOI
16. Lundberg SM, Lee SI. A unified approach to interpreting model predictions. Available from: https://proceedings.neurips.cc/paper/2017/hash/8a20a8621978632d76c43dfd28b67767-Abstract.html [Last accessed on 22 Dec 2022]
17. Vo TH, Nguyen NTK, Kha QH, Le NQK. On the road to explainable AI in drug-drug interactions prediction: a systematic review. *Comput Struct Biotechnol J* 2022;20:2112-23. DOI
18. Kha QH, Tran TO, Nguyen VN, et al. An interpretable deep learning model for classifying adaptor protein complexes from sequence information. *Methods* 2022;207:90–96. DOI
19. Durán JM. Dissecting scientific explanation in AI (sXAI): a case for medicine and healthcare. *Art Int* 2021;297:103498. DOI
20. Shaban-Nejad A, Michalowski M, Buckeridge DL. Explainability and interpretability: keys to deep medicine. In: Explainable AI in Healthcare and Medicine. Springer; 2021. pp. 1–10.
21. Naser M. Deriving mapping functions to tie anthropometric measurements to body mass index via interpretable machine learning. Machine Learning with Applications 2022;8:100259. DOI

22. Bhandari M, Shahi TB, Siku B, Neupane A. Explanatory classification of CXR images into COVID-19, Pneumonia and Tuberculosis using deep learning and XAI. *Comput Biol Med* 2022;150:106156. DOI
23. Lombardi A, Tavares JMR, Tangaro S. Explainable Artificial Intelligence (XAI) in Systems Neuroscience. *Front Syst Neurosci* 2021;15. DOI
24. Abdel-Zaher AM, Eldeib AM. Breast cancer classification using deep belief networks. *Expert Systems with Applications* 2016;46:139–44. DOI
25. UCI Machine Learning Repository: Breast Cancer Wisconsin (diagnostic) data set;. Accessed: 2022-07-13. Available from: https://archive.ics.uci.edu/ml/datasets/breast+cancer+wisconsin+(diagnostic) [Last accessed on 22 Dec 2022]
26. Ribeiro MT, Singh S, Guestrin C. "Why should I trust you?": Explaining the predictions of any classifier. In: Proceedings of the 22nd ACM SIGKDD International Conference on Knowledge Discovery and Data Mining, San Francisco, CA, USA, August 13-17, 2016; 2016. pp. 1135–44.
27. An introduction to explainable AI with Shapley values;. Accessed: 2022-07-15. Available from: https://towardsdatascience.com/shap-explained-the-way-i-wish-someone-explained-it-to-me-ab81cc69ef30. [Last accessed on 22 Dec 2022]
28. Paszke A, Gross S, Massa F, et al. PyTorch: An imperative style, high-performance deep learning library. In: Wallach H, Larochelle H, Beygelzimer A, d'Alché-Buc F, Fox E, et al., editors. Advances in Neural Information Processing Systems 32. Curran Associates, Inc.; 2019. pp. 8024–35. Available from: http://papers.neurips.cc/paper/9015-pytorch-an-imperative-style-high-performance-deep-learning-library.pdf [Last accessed on 22 Dec 2022]
29. Kadam VJ, Jadhav SM, Vijayakumar K. Breast cancer diagnosis using feature ensemble learning based on stacked sparse autoencoders and softmax regression. *J Med Syst* 2019;43:1–11. DOI
30. Street WN, Wolberg WH, Mangasarian OL. Nuclear feature extraction for breast tumor diagnosis. In: Biomedical image processing and biomedical visualization. vol. 1905. SPIE; 1993. pp. 861–70.
31. Hariharan S, Rejimol Robinson R, Prasad RR, Thomas C, Balakrishnan N. XAI for intrusion detection system: comparing explanations based on global and local scope. *J Comput Virol Hack Tech* 2022:1–23. DOI
32. Visani G, Bagli E, Chesani F, Poluzzi A, Capuzzo D. Statistical stability indices for LIME: Obtaining reliable explanations for machine learning models. *J Operatl Res Society* 2022;73:91–101. DOI
33. Magesh PR, Myloth RD, Tom RJ. An explainable machine learning model for early detection of Parkinson's disease using LIME on DaTSCAN imagery. *Comput Biol Med* 2020;126:104041. DOI

Sun *et al. Complex Eng Syst* 2022;2:17
DOI: 10.20517/ces.2022.48

Complex Engineering Systems

Research Article

Open Access

Stability analysis for highly nonlinear switched stochastic systems with time-varying delays

Jing Sun[1], Hui Wang[1,2,3]

[1]School of Mathematics and Statistics, Nanjing University of Information Science and Technology, Nanjing 210044, Jiangsu, China.
[2]Center for Applied Mathematics of Jiangsu Province, Nanjing University of Information Science and Technology, Nanjing 210044, Jiangsu, China.
[3]Jiangsu International Joint Laboratory on System Modeling and Data Analysis, Nanjing University of Information Science and Technology, Nanjing 210044, Jiangsu, China.

Correspondence to: Dr. Hui Wang, School of Mathematics and Statistics, Nanjing University of Information Science and Technology, No. 219 Ningliu Road, Nanjing 210044, Jiangsu, China. E-mail: wang_8063085@163.com

How to cite this article: Sun J, Wang H. Stability analysis for highly nonlinear switched stochastic systems with time-varying delays. *Complex Eng Syst* 2022;2:17. http://dx.doi.org/10.20517/ces.2022.48

Received: 11 Nov 2022 **First Decision:** 30 Nov 2022 **Revised:** 19 Dec 2022 **Accepted:** 21 Dec 2022 **Published:** 27 Dec 2022

Academic Editor: Hamid Reza Karimi **Copy Editor:** Fanglin Lan **Production Editor:** Fanglin Lan

Abstract

In this paper, we examine the stability of highly nonlinear switched stochastic systems (SSSs) with time-varying delays, where the switching time instants are deterministic rather than stochastic. Herein, the boundedness of the global solution is first proven for highly nonlinear SSSs via the average dwell time (ADT) method and multiple Lyapunov function (MLF) approach. Then, the stability criteria for qth moment exponential stability and almost surely exponential stability are presented. The main difficulty lies in the presence of switching and time-varying delay terms, which prevents the validation of existing methods. New inequality techniques have been developed to counteract the effects of switching signals and time-varying delays. Finally, an example is provided to verify the effectiveness of the results.

Keywords: Highly nonlinear switched stochastic systems, deterministic switching signal, time-varying delays, average dwell time, multiple Lyapunov function

1. INTRODUCTION

Switched systems are important dynamic systems. The idea of switching has been widely applied in various fields, such as aircraft attitude control[1], ecological dynamics[2], and financial markets[3]. With the increasing complexity of system architectures, dynamical analysis of switched systems has attracted significant academic interest. A switched system consists of a family of continuous-time dynamics, discrete-time dynamics, and switching rules between subsystems. According to the switching signal features, switched systems are divided into two categories, *namely*, deterministic switched systems and randomly switched systems. Many researchers have focused on stabilization and stability analyses of various switched systems. For example, in[4], a series of results on stochastic differential equations (SDEs) with Markovian switching was obtained. In particular, the authors have provided some useful stability criteria. In[5], the authors studied the input-to-state stability of time-varying switched systems by employing the ADT method coupled with the MLF approach. The authors of[6] investigated the stability of switched stochastic delay neural networks with all unstable subsystems based on discretized Lyapunov-Krasovskii functions (DLKFs). In[7], a novel Lyapunov function was designed to ensure a non-weighted $\mathcal{L}_2$ gain for switched systems with asynchronous switching. In[8], a hidden Markov model was proposed to study the finite region H_∞ asynchronous control problem for two-dimensional Markov jump systems. Other interesting researches on switched systems can be found in[9–11] and references therein.

The linear growth condition (LGC) is crucial for ensuring the existence of a global solution for a stochastic system. However, many stochastic systems do not satisfy LGC. Hence, the solution of a stochastic system may explode in a finite time. Recently, the stability of stochastic systems without LGC has drawn considerable attention. For instance, the authors of[12] investigated the stability and boundedness of nonlinear hybrid stochastic differential delay equations without LGC based on a Lyapunov function approach. By introducing a polynomial growth condition (PGC),[13] discussed the stabilization problem of highly nonlinear hybrid SDEs. The input-to-state practically exponential stability in the sense of mean square was introduced in[14]. Sufficient conditions for stability have been obtained. Additionally, other meaningful results were reported in[15] and[16].

Time-delay is an important factor that affects dynamical performances of stochastic systems. By constructing a suitable Lyapunov function, the authors of[12] studied the stability and boundedness of highly nonlinear hybrid stochastic systems with a time delay. The authors of[17] used the ADT method to study the stability problem of SSSs, where the switching signals are deterministic. Based on the stability criteria for stochastic time-delay systems, the authors of[18] introduced a suitable Lyapunov-Krasovskii (L-K) functional, and discussed the global probabilistic asymptotic stability of the closed-loop system. In[19], the Razumikhin approach was presented to study the exponential stability of a class of impulsive stochastic delay differential systems. Using the piecewise dynamic gain method, the authors of[20] studied the global uniform ultimate boundedness of switched linear time-delay systems. Motivated by the aforementioned literature, the stability of highly nonlinear SSSs with time-varying delays is studied in this paper. Figure 1 shows the framework of this paper.

The challenges of this article lie in the following two parts: (1) The time delay studied here is merely a Borel measurable function of time t. That is to say, it may be non-differentiable with respect to time t, which means that the existing methods regarding constant delays or differentiable delays are no longer applicable; (2) Rather than a Markovian switching signal, a deterministic switching signal is involved in the studied system, indicating that Markovian switched systems based M-matrix method is invalid. To address the influences of deterministic switching signals, an ADT method coupled with the MLF approach is utilized in our stability analysis.

The main advantages of this paper are as follows:
(1) Without the LGC, the existence and uniqueness of a global solution is proven for highly nonlinear SSSs, where a deterministic switching signal rather than a Markovian switching signal is considered.
(2) By integrating the ADT method and MLF approach, the qth moment exponential stability and almost

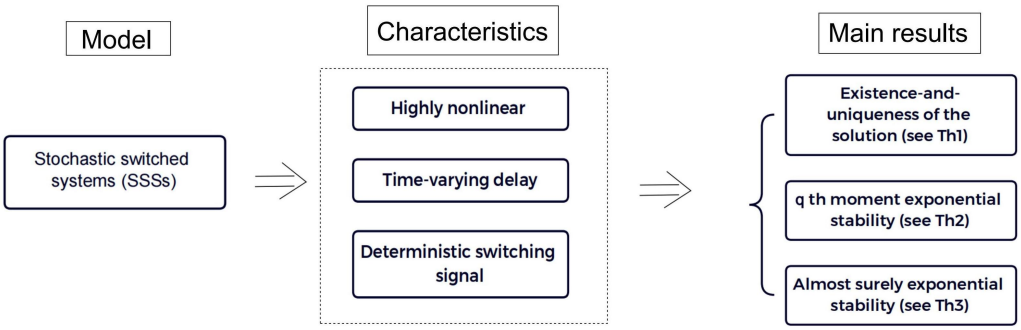

Figure 1. Framework of the paper.

surely exponential stability are presented for highly nonlinear SSSs with time-varying delays.

The remainder of this paper is organized as follows. An introduction of the model and important assumptions are given in Section 2. The existence of a unique global solution and stability analysis are presented in Sections 3. In Section 4, a simulation example is presented to validate our theoretical results. Finally, Section 5 concludes the paper.

Note: In this paper, $\mathbb{R}_+ = (0, \infty)$, $\mathbb{N}_+ = 1, 2, \cdots, \kappa, \cdots$, $\mathbb{N} = \mathbb{N}_+ \cup \{0\}$ with κ being a positive finite integer, $\mathbb{R}^n$ denotes the n-dimensional real space. For $x \in \mathbb{R}^n$, $|x| = \left(\sum_{i=1}^n x_i^2\right)^{\frac{1}{2}}$ denotes the Euclidean norm of vector. For any matrix $A \in \mathbb{R}^{n\times n}$, $|A| = \sqrt{A^T A}$ denotes the trace norm of matrix A, where A^T is the transpose of matrix A and $\mathrm{tr}\{A\}$ denotes its trace. For $\tau > 0$, $C([-\tau, 0]; \mathbb{R}^n)$ denotes the space of all continuous functions φ from $[-\tau, 0] \to \mathbb{R}^n$ with the norm $||\varphi|| = \sup_{-\tau\le u\le 0} |\varphi(u)|$, $C^b_{\mathcal{F}_0}([-\tau, 0]; \mathbb{R}^n)$ denotes the family of all $\mathcal{F}_0$-measurable bounded $C([-\tau, 0]; \mathbb{R}^n)$-valued random variable $\xi = \{\xi(\theta) : -\tau \le \theta \le 0\}$. Let $(\Omega, \mathcal{F}, \mathbb{P})$ be a complete probability space with a filtration $\{\mathcal{F}_t\}_{t\ge 0}$. $B(t)$=$(B_1(t), \cdots, B_m(t))$ denotes an m-dimensional $\mathcal{F}_t$-adapted Brownian motion, which is defined on a complete probability space. In addition, $\mathcal{V}^{1,2}$ denotes the family of all non-negative functions $V(t, x, i) : [-\tau, \infty) \times \mathbb{R}^n \times \Gamma \to \mathbb{R}_+$, which are first-order continuously differentiable in t and second-order continuously differentiable in x. Let $C([-\tau, \infty) \times \mathbb{R}^n; \mathbb{R}_+)$ be the family of continuous functions $W : [-\tau, \infty) \times \mathbb{R}^n \to \mathbb{R}_+$. For real numbers a and b, $a \wedge b = \min\{a, b\}$, $a \vee b = \max\{a, b\}$.

2. PRELIMINARIES

Model descriptions and assumptions are introduced in this section. In this study, we analyzed the following highly nonlinear SSS with time-varying delays:

$$dx(t) = f_{\sigma(t)}(t, x(t), x(t - \delta_t))dt + g_{\sigma(t)}(t, x(t), x(t - \delta_t))dB(t), \tag{1}$$

with the initial value:

$$\{x(t) : -m \le t \le 0\} = \xi \in C^b_{\mathcal{F}_0}([-m, 0]; \mathbb{R}^n), \tag{2}$$

where $m > 0$ is a constant and switching signal $\sigma(t) : [0, \infty) \to \Gamma = \{1, 2, \cdots, \kappa\}$ is a piecewise constant function that is continuous from the right. In particular, it is a non-random function of t. For $t \in [t_m, t_{m+1})$, $\sigma(t) = i_m \in \Gamma$, where t_m is the mth switching time instant and $m \in \mathbb{N}$. For each $i \in \Gamma$, the mappings $f_i : \mathbb{R}^+ \times \mathbb{R}^n \times \mathbb{R}^n \to \mathbb{R}^n$ and $g_i : \mathbb{R}^+ \times \mathbb{R}^n \times \mathbb{R}^n \to \mathbb{R}^{n\times m}$ are Borel-measurable functions. Compared with [13], one of the merits of this paper is that the time delay δ_t is merely a Borel measurable function of t and may be non-differentiable. Precisely, we need to impose some requirements on the time-varying delay δ_t.

Assumption 1 *The time-varying delay δ_t is a Borel measurable function of t from $\mathbb{R}_+ \to [m_1, m]$ with the property that*

$$\bar{m} = \limsup_{\Delta \to 0_+} \left(\sup_{s \geq -m} \frac{\mu(M_{s,\Delta})}{\Delta} \right) < \infty, \tag{3}$$

where m_1 and m are positive constants, $M_{s,\Delta} = \{t \in \mathbb{R}_+ : t - \delta_t \in [s, s + \Delta)\}$ and $\mu(\cdot)$ denotes the Lebesgue measure on $\mathbb{R}_+$.

Remark 1 *Assumption 1 reveals that the time delay in SSS (1) is merely a Borel measurable function of time t, which means that it may be non-differentiable with respect to time t. In most reported studies on SSSs (see, e.g., [21–25]), the time delay δ_t is always assumed to be a differentiable function and its time derivative $\dot{\delta}_t$ should satisfy $\dot{\delta}_t \leq \bar{\delta} < 1$ with $\bar{\delta}$ being a positive constant. However, this condition is too conservative for practical application. Many time-delay functions in actual systems do not satisfy this assumption. For example, a time-varying delay δ_t is defined as $\delta_t = 0.5 + 0.25|\sin(10t)|$. If δ_t is a Lipschitz continuous function with a Lipschitz coefficient $m_2 \in (0, 1)$, namely, $|\delta_t - \delta_s| \leq m_2|t - s|$, then for all $0 \leq s < t < \infty$. Then, δ_t satisfies Assumption 1 with $\bar{m} = (1 - m_2)^{-1}$. In particular, if δ_t is differentiable and its derivative is bounded by $m_2 \in (0, 1)$, then δ_t still satisfies Assumption 1. From a theoretical perspective, a large class of functions δ_t can satisfy Assumption 1. Note that the constant $\bar{m}$ must not be less than 1 (i.e., $\bar{m} \geq 1$). This point can be obtained from the following lemma, with $\psi = 1$.*

The following lemma provides a useful inequality to obtain the stability of the SSS (1) with time-varying delays, and its proof can be found in [16].

Lemma 1 [16] *Let $T > 0$ and $\psi : [t_0 - m, T - m_1] \to \mathbb{R}^+$ be a continuous function. If Assumption 1 holds, then*

$$\int_{t_0}^{T} \psi(t - \delta_t)dt \leq \bar{m} \int_{t_0 - m}^{T - m_1} \psi(t)dt. \tag{4}$$

The conditions for the existence and uniqueness of global solution are the local Lipschitz condition (LLC) and the LGC (see, e.g., [4,7,20,26]). In this paper, the highly nonlinear SSS (1) generally does not require the LGC. Consequently, we must impose the PGC on it.

Assumption 2 *(LLC & PGC) For any real number $b > 0, i \in \Gamma$, there exists a constant $K_{b,i} > 0$ such that*

$$|f_i(t, x, y) - f_i(t, \bar{x}, \bar{y})| \vee |g_i(t, x, y) - g_i(t, \bar{x}.\bar{y})| \leq K_{b,i}(|x - \bar{x}| + |y - \bar{y}|), \tag{5}$$

for all $x, \bar{x}, y, \bar{y} \in \mathbb{R}^n$, where $|x| \vee |\bar{x}| \vee |y| \vee |\bar{y}| \leq b$. Moreover, there exist constants $K > 0, \alpha_1 > 1, \alpha_2 \geq 1$ such that

$$\begin{aligned} |f_i(t, x, y)| &\leq K(1 + |x|^{\alpha_1} + |y|^{\alpha_1}), \\ |g_i(t, x, y)| &\leq K(1 + |x|^{\alpha_2} + |y|^{\alpha_2}), \end{aligned} \tag{6}$$

where $(t, x, y) \in \mathbb{R}^+ \times \mathbb{R}^n \times \mathbb{R}^n$ and $i \in \Gamma$.

Assumption 3 *Assume that there are two functions $\Lambda \in \mathcal{V}^{1,2}([-m, \infty) \times \mathbb{R}^n \times \Gamma; \mathbb{R}_+)$ and $W \in C([-m, \infty) \times \mathbb{R}^n; \mathbb{R}_+)$, as well as positive numbers $a_1, a_2, \lambda_1, \lambda_3$ and real numbers λ_2, λ_4, satisfying $\lambda_1 > \lambda_2, \lambda_3 > \lambda_4$ and $q > 2, \mu_i > 1$, such that for any $(t, x, y, i) \in \mathbb{R}_+ \times \mathbb{R}^n \times \mathbb{R}^n \times \Gamma$,*

$$a_1|x|^q \leq \Lambda(t, x, i) \leq a_2|x|^q, \tag{7}$$

$$\Lambda(t, x, i) \leq \mu_i \Lambda(t, x, j), \quad \forall (t, x, i) \in \mathbb{R}_+ \times \mathbb{R}^n \times \Gamma, \tag{8}$$

$$\begin{aligned} \mathcal{L}\Lambda(t, x, y, i) &= \Lambda_t(t, x, i) + \Lambda_x(t, x, i) f_i(t, x, y) + \frac{1}{2}\text{trace}\{{g_i}^T(t, x, y)\Lambda_{xx}(t, x, i)g_i(t, x, y)\} \\ &\leq -\lambda_1 W(x) + \lambda_2 W(y) - \lambda_3|x|^q + \lambda_4|y|^q, \end{aligned} \tag{9}$$

where $y = x(t-\delta_t)$ *and*

$$\Lambda_t(t,x,i) = \frac{\partial \Lambda(t,x,i)}{\partial t},$$
$$\Lambda_x(t,x,i) = \left(\frac{\partial \Lambda(t,x,i)}{\partial x_1}, \cdots, \frac{\partial \Lambda(t,x,i)}{\partial x_n}\right),$$
$$\Lambda_{xx}(t,x,i) = \left(\frac{\partial^2 \Lambda(t,x,i)}{\partial x_j \partial x_k}\right)_{n\times n}.$$

Moreover, assume that there exists a constant $\varepsilon > 0$*, such that*

$$\lambda_3 - \lambda_4 \bar{m} e^{\varepsilon m} - \varepsilon a_2 = 0, \tag{10}$$
$$\lambda_1 - \lambda_2 \bar{m} e^{\varepsilon m} > 0. \tag{11}$$

Remark 2 *The system studied in this research has the property of high nonlinearity. In other words, the LGC is removed from the SSS (1), which makes the considered system more general. Without the LGC, the solution of a stochastic system may explode in a finite time. To ensure the existence of a global solution, a PGC (i.e., condition (6)) is imposed on the SSS (1) (see, e.g.,* [13,27,28]*). Therefore, the system (1) we studied obeys the LLC (i.e., condition (5)) and the PGC. By combining the MLF approach and ADT method, we then prove the existence and uniqueness of the global solution.*

Before presenting the main results, the definition of ADT is revisited.

Definition 1 [28] *For a switching signal* $\sigma(t)$ *and any* $t \geq s \geq 0$*,* $T_i(t,s)$ *and* $N_i(t,s)$ *denote the whole running time and the switching number of the i-th subsystem over the interval* $[s,t]$*, respectively,* $i \in \Gamma$*. Then, the following inequality holds:*

$$N_i(t,s) \leq \frac{T_i(t,s)}{\mathcal{J}_{ai}} + N_{0i},$$

where $\mathcal{J}_{ai} > 0$ *is called the mode-dependent ADT and* $N_{0i} > 0$ *is the mode-dependent chatter bound.*

3. MAIN RESULTS

In this section, we prove the existence of a unique global solution for a highly nonlinear SSS (1) by using the ADT and MLF approaches. Then, both the qth moment exponential stability and almost surely exponential stability are provided for a highly nonlinear SSS (1).

Theorem 1 *Under Assumptions 1-3, if there exists a constant* $\varepsilon > 0$ *such that*

$$\mathcal{J}_{ai} > \frac{\ln \mu_i}{\varepsilon}. \tag{12}$$

Then, for any initial data (2), there exists a unique global solution $x(t)$ *for the SSS (1) on* $[-m,\infty)$*, and the solution satisfies*

$$\sup_{-m\leq t<\infty} E|x(t)|^q < \infty. \tag{13}$$

Proof. We divide the whole proof into two steps. In step 1, for all $i \in \mathbb{S}$, we prove that the i-th subsystem with the initial value $x_i(0)$ has a unique global solution $x_i(t)$. In step 2, when each subsystem has a unique global solution, the SSS (1) with a deterministic switching signal has a unique global solution $x(t)$ on $[-m,\infty)$.
Step 1. For all $i \in \mathbb{S}$, the control system becomes

$$dx_i(t) = f_i(t,x_i(t),y_i(t))dt + g_i(t,x_i(t),y_i(t))dB(t), \quad t \geq -m, \tag{14}$$

where $y_i(t) = x_i(t-\delta_t)$. Under the LLC, system (14) has a unique maximal global solution on $[-m, \rho_\infty^i)$, denoted as $x_i(t)$, where ρ_∞^i is the explosion time. Then, we prove $\rho_\infty^i = \infty$ a.s. Thus, it is necessary to define the stopping time sequence. Let k_0 be a constant sufficiently large to satisfy $k_0 > |x_i(0)|$. For any integer $k \geq k_0$, we define the stopping time sequence as follows:

$$\delta_{k,i} = \inf\{t \in [0, \rho_\infty^i), |x_i(t)| \geqslant k\}.$$

Clearly , $\delta_{k,i}$ increases as $k \to \infty$ and therefore we set $\delta_{\infty,i} := \lim_{k\to\infty} \delta_{k,i}$. Observe that $\delta_{\infty,i} \leq \rho_{\infty,i}$ a.s. Thus, $\delta_{\infty,i} = \infty$, a.s., which yields $\rho_{\infty,i} = \infty$ a.s. From the Itô formula and condition (9), it is easily proven that

$$\begin{aligned}
&Ee^{\varepsilon(t\wedge\delta_{k,i})}\Lambda(t\wedge\delta_{k,i}, x_i(t\wedge\delta_{k,i}), i)\\
&= Ee^{\varepsilon t_0}\Lambda(t_0, x_i(t_0), i) + E\int_{t_0}^{t\wedge\delta_{k,i}} e^{\varepsilon s}[\varepsilon\Lambda(s, x_i(s), i) + \mathcal{L}\Lambda(s, x_i(s), i)]ds\\
&\leq Ee^{\varepsilon t_0}\Lambda(t_0, x_i(t_0), i) + E\int_{t_0}^{t\wedge\delta_{k,i}} e^{\varepsilon s}[\varepsilon a_2|x_i(s)|^q - \lambda_1 W(x_i(s)) + \lambda_2 W(y_i(s))\\
&\quad - \lambda_3|x_i(s)|^q + \lambda_4|y_i(s)|^q]ds.
\end{aligned}$$

By Lemma 1, we have

$$\begin{aligned}
&E\int_{t_0}^{t\wedge\delta_{k,i}} e^{\varepsilon s}W(x_i(s-\delta_s))ds\\
&\leq e^{\varepsilon m}\bar{m}E\int_{t_0-m}^{t\wedge\delta_{k,i}} e^{\varepsilon s}W(x_i(s))ds\\
&\leq e^{\varepsilon m}\bar{m}E\int_{t_0-m}^{t_0} e^{\varepsilon s}W(x_i(s))ds + e^{\varepsilon m}\bar{m}E\int_{t_0}^{t\wedge\delta_{k,i}} e^{\varepsilon s}W(x_i(s))ds,
\end{aligned} \tag{15}$$

and

$$\begin{aligned}
&E\int_{t_0}^{t\wedge\delta_{k,i}} e^{\varepsilon s}|x_i(s-\delta_s)|^q ds\\
&\leq e^{\varepsilon m}\bar{m}E\int_{t_0-m}^{t\wedge\delta_{k,i}} e^{\varepsilon s}|x_i(s)|^q ds\\
&\leq e^{\varepsilon m}\bar{m}E\int_{t_0-m}^{t_0} e^{\varepsilon s}|x_i(s)|^q ds + e^{\varepsilon m}\bar{m}E\int_{t_0}^{t\wedge\delta_{k,i}} e^{\varepsilon s}|x_i(s)|^q ds.
\end{aligned} \tag{16}$$

Hence,

$$\begin{aligned}
&Ee^{\varepsilon(t\wedge\delta_{k,i})}\Lambda(t\wedge\delta_{k,i}, x_i(t\wedge\delta_{k,i}), i)\\
&\leq C - (\lambda_3 - \lambda_4\bar{m}e^{\varepsilon m} - \varepsilon a_2)E\int_{t_0}^{t\wedge\delta_{k,i}} e^{\varepsilon s}|x_i(s)|^q ds - (\lambda_1 - \lambda_2\bar{m}e^{\varepsilon m})E\int_{t_0}^{t\wedge\delta_{k,i}} e^{\varepsilon s}W(x_i(s))ds,
\end{aligned}$$

where

$$\begin{aligned}
C =& E\left(\sup_{[t_0-m,t_0]} e^{\varepsilon t_0}\Lambda(t_0, \xi, i)\right) + \lambda_2\bar{m}e^{\varepsilon m}E\left(\sup_{[t_0-m,t_0]}\int_{t_0-m}^{t_0} e^{\varepsilon t_0}W(\xi)ds\right)\\
&+ \lambda_4\bar{m}e^{\varepsilon m}E\left(\sup_{[t_0-m,t_0]}\int_{t_0-m}^{t_0} e^{\varepsilon t_0}|\xi|^q ds\right)
\end{aligned}$$

is a finite constant. Applying (10) and (11) from Assumption 3, we can deduce that

$$Ee^{\varepsilon(t\wedge\delta_{k,i})}\Lambda(t\wedge\delta_{k,i}, x_i(t\wedge\delta_{k,i}), i) \leq C.$$

Recalling the condition (7), we can get

$$Ea_1 e^{\varepsilon(t\wedge\delta_{k,i})}|x_i(t\wedge\delta_{k,i})|^q \le C.$$

This implies

$$k^q P(\delta_{k,i}\le t) \le E|x_i(t\wedge\delta_{k,i})|^q \le \frac{C}{a_1}e^{-\varepsilon(t\wedge\delta_{k,i})}.$$

We observe that

$$P(\delta_{k,i}\le t) \le \frac{C}{a_1 k^q}e^{-\varepsilon(t\wedge\delta_{k,i})}.$$

Letting $k\to\infty$ yields that $P(\delta_{\infty,i}\leqslant t)=0$. Hence, $\delta_{\infty,i}=\infty$ a.s. Therefore, we have $\rho_{\infty,i}=\infty$ a.s. This implies that the unique solution for the i-th subsystem (14) will not explode in finite time.

Step 2. This section proves the existence of a unique global solution for SSS (1). Let $k_0>0$ be a sufficiently large integer, such that $k_0>|x_i(0)|$, where $|x_i(0)|$ is the initial data of the i-th subsystem. For any integer $k\ge k_0$, we define the stopping time sequence as follows:

$$\delta_k^n = \inf\{t\in[t_n,t_{n+1}) : |x(t)|\geqslant k\}.$$

Clearly, δ_k^n increases as $k\to\infty$. For $t\in[t_0,t_1)$, $\sigma(t)=i_0$, using the Itô formula, we have

$$\begin{aligned} &Ee^{\varepsilon(t\wedge\delta_k^0)}\Lambda(t\wedge\delta_k^0,x(t\wedge\delta_k^0),i_0)\\ &\le Ee^{\varepsilon t_0}\Lambda(t_0,x(t_0),i_0)+E\int_{t_0}^{t\wedge\delta_k^0}e^{\varepsilon s}\Xi(s,i_0)ds, \end{aligned} \tag{17}$$

where $\Xi(s,i_0)=\varepsilon\Lambda(s,x(s),i_0)+\mathcal{L}\Lambda(s,x(s),y(s),i_0)$. Letting $t=t_1$, according to condition (8) in Assumption 3, we derive that

$$\begin{aligned} &Ee^{\varepsilon t_1}\Lambda(t_1,x(t_1),i_1)\le\mu_i Ee^{\varepsilon t_1}\Lambda(t_1,x(t_1),i_0)\\ &\le\mu_i[Ee^{\varepsilon t_0}\Lambda(t_0,x(t_0),i_0)+E\int_{t_0}^{t_1}e^{\varepsilon s}\Xi(s,i_0)ds]. \end{aligned} \tag{18}$$

For $t\in[t_1,t_2)$, $\sigma(t)=i_1$, we obtain

$$\begin{aligned} &Ee^{\varepsilon(t\wedge\delta_k^1)}\Lambda(t\wedge\delta_k^1,x(t\wedge\delta_k^1),i_1)\\ &\le Ee^{\varepsilon t_1}\Lambda(t_1,x(t_1),i_1)+E\int_{t_1}^{t\wedge\delta_k^1}e^{\varepsilon s}\Xi(s,i_1)ds. \end{aligned} \tag{19}$$

Combining (18) and (19), it implies that

$$\begin{aligned} &Ee^{\varepsilon(t\wedge\delta_k^1)}\Lambda(t\wedge\delta_k^1,x(t\wedge\delta_k^1),i_1)\\ &\le\mu_i[Ee^{\varepsilon t_0}\Lambda(t_0,x(t_0),i_0)+E\int_{t_0}^{t_1}e^{\varepsilon s}\Xi(s,i_0)ds]+E\int_{t_1}^{t\wedge\delta_k^1}e^{\varepsilon s}\Xi(s,i_1)ds. \end{aligned} \tag{20}$$

For $t\in[t_{m-1},t_m)$ and $\sigma(t)=i_{m-1}$, we assume that

$$\begin{aligned} &Ee^{\varepsilon(t\wedge\delta_k^{m-1})}\Lambda(t\wedge\delta_k^{m-1},x(t\wedge\delta_k^{m-1}),i_{m-1})\\ &\le Ee^{\varepsilon t_{m-1}}\Lambda(t_{m-1},x(t_{m-1}),i_{m-1})+E\int_{t_{m-1}}^{t\wedge\delta_k^{m-1}}e^{\varepsilon s}\Xi(s,i_{m-1})ds\\ &\le\mu_i^{N_i(t_{m-1},t_0)}Ee^{\varepsilon t_0}\Lambda(t_0,x(t_0),i_0)+\mu_i^{N_i(t_{m-1},t_0)}E\int_{t_0}^{t_1}e^{\varepsilon s}\Xi(s,i_0)ds\\ &+\mu_i^{N_i(t_{m-1},t_0)-1}E\int_{t_1}^{t_2}e^{\varepsilon s}\Xi(s,i_1)ds+\cdots+\mu_iE\int_{t_{m-2}}^{t_{m-1}}e^{\varepsilon s}\Xi(s,i_{m-2})ds\\ &+E\int_{t_{m-1}}^{t\wedge\delta_k^{m-1}}e^{\varepsilon s}\Xi(s,i_{m-1})ds. \end{aligned} \tag{21}$$

By mathematical induction, for $t \in [t_m, t_{m+1})$ and $\sigma(t) = i_m$, we have

$$Ee^{\varepsilon(t\wedge\delta_k^m)}\Lambda(t\wedge\delta_k^m, x(t\wedge\delta_k^m), i_m) = Ee^{\varepsilon t_m}\Lambda(t_m, x(t_m), i_m) + E\int_{t_m}^{t\wedge\delta_k^m} e^{\varepsilon s}\Xi(s, i_m)ds. \tag{22}$$

It follows from (8) and (21) that

$$\begin{aligned}
&Ee^{\varepsilon(t\wedge\delta_k^m)}\Lambda(t\wedge\delta_k^m, x(t\wedge\delta_k^m), i_m)\\
&\le \mu_i Ee^{\varepsilon t_m}\Lambda(t_m, x(t_m), i_{m-1}) + E\int_{t_m}^{t\wedge\delta_k^m} e^{\varepsilon s}\Xi(s, i_m)ds\\
&\le \mu_i^{N_i(t_m,t_0)}Ee^{\varepsilon t_0}\Lambda(t_0, x(t_0), i_0) + \mu_i^{N_i(t_m,t_0)}E\int_{t_0}^{t_1} e^{\varepsilon s}\Xi(s, i_0)ds + \cdots\\
&+ \mu_i^2 E\int_{t_{m-2}}^{t_{m-1}} e^{\varepsilon s}\Xi(s, i_{m-2})ds + \mu_i E\int_{t_{m-1}}^{t_m} e^{\varepsilon s}\Xi(s, i_{m-1})ds + E\int_{t_m}^{t\wedge\delta_k^m} e^{\varepsilon s}\Xi(s, i_m)ds.
\end{aligned} \tag{23}$$

Because $\mu_i > 1$, we obtain from (23) that

$$Ee^{\varepsilon(t\wedge\delta_k^m)}\Lambda(t\wedge\delta_k^m, x(t\wedge\delta_k^m), i_m) \le \mu_i^{N_i(t,t_0)}[Ee^{\varepsilon t_0}\Lambda(t_0, x(t_0), i_0) + E\int_{t_0}^{t\wedge\delta_k^m} e^{\varepsilon s}\Xi(s, i_m)ds].$$

Similar to the proof stated in Part 1, we can derive

$$\begin{aligned}
Ee^{\varepsilon(t\wedge\delta_k^m)}\Lambda(t\wedge\delta_k^m, x(t\wedge\delta_k^m), i_m) \le \mu_i^{N_i(t,t_0)}[&C_1 - (\lambda_1 - \lambda_2\bar{m}e^{\varepsilon m})E\int_{t_0}^{t\wedge\delta_k^m} e^{\varepsilon s}W(x(s))ds\\
&- (\lambda_3 - \lambda_4\bar{m}e^{\varepsilon m} - \varepsilon a_2)E\int_{t_0}^{t\wedge\delta_k^m} e^{\varepsilon s}|x(s)|^q ds],
\end{aligned}$$

where

$$\begin{aligned}
C_1 =&E\left(\sup_{[t_0-m,t_0]} e^{\varepsilon t_0}\Lambda(t_0, \xi, i_0)\right) + \lambda_2\bar{m}e^{\varepsilon m}E\left(\sup_{[t_0-m,t_0]}\int_{t_0-m}^{t_0} e^{\varepsilon t_0}W(\xi)ds\right)\\
&+ \lambda_4\bar{m}e^{\varepsilon m}E\left(\sup_{[t_0-m,t_0]}\int_{t_0-m}^{t_0} e^{\varepsilon t_0}|\xi|^q ds\right),
\end{aligned}$$

is finite. Then,

$$Ee^{\varepsilon(t\wedge\delta_k^m)}\Lambda(t\wedge\delta_k^m, x(t\wedge\delta_k^m), i_m) \le C_1\mu_i^{N_i(t,t_0)}. \tag{24}$$

Recalling condition (7), we obtain

$$E|x(t\wedge\delta_k^m)|^q \le \frac{C_1}{a_1}\mu_i^{N_i(t,t_0)}e^{-\varepsilon(t\wedge\delta_k^m)}.$$

This implies

$$P(\delta_k^m \le t) \le \frac{C_1}{a_1 k^q}\mu_i^{N_i(t,t_0)}e^{-\varepsilon(t\wedge\delta_k^m)}.$$

Letting $k \to \infty$, we observe that $P(\delta_\infty^m \le t) = 0$ and hence $\delta_\infty^m \ge t$ a.s. We let $k \to \infty$ in (24) to obtain

$$E\Lambda(t, x(t), \sigma(t)) \le \mu_i^{N_i(t,t_0)}C_1 e^{-\varepsilon t}.$$

Using Definition 1, we have that for $t \geq 0$ and $i \in \Gamma$,

$$\begin{aligned} E\Lambda(t, x(t), \sigma(t)) &\leq C_1 \mu_i^{\frac{t-t_0}{\mathcal{T}_{ai}}+N_{0i}} e^{-\varepsilon t} \\ &\leq C_1 \mu_i^{N_{0i}} e^{\frac{\ln \mu_i}{\mathcal{T}_{ai}} t} e^{-\varepsilon t} \\ &= C_2 e^{-\left(\varepsilon - \frac{\ln \mu_i}{\mathcal{T}_{ai}}\right) t}, \end{aligned} \tag{25}$$

where $C_2 = C_1 \mu_i^{N_{0i}}$. This implies

$$E|x(t)|^q \leq \frac{C_2}{a_1}. \tag{26}$$

Therefore, for all $m \in \mathbb{N}$, we obtain

$$E\Lambda(t_m, x(t_m), \sigma(t_m)) \leq C_2.$$

This means that the unique solution $x(t)$ will not explode for $t \in [t_m, t_{m+1})$ and $m \in \mathbb{N}$. Hence, there exists a unique global solution $\{x(t), t \geq 0\}$ for SSS (1). Moreover, from (25), we obtain that

$$\sup_{-m \leq t \leq \infty} \mathrm{E}|x(t)|^q < \infty.$$

The proof is completed. □

Remark 3 *To deal with the time-varying delay δ_t, some new inequalities (e.g., see (15) and (16) for details) are constructed in the proof for Theorem 1. Compared with the results reported in existing studies[21–25], the time delay δ_t in this paper is merely a Borel-measurable function, which invalidates these existing methods. By virtue of Lemma 1, a more general form of time delay can be imposed on system (1).*

We now refer to the equation (25) in the proof of Theorem 1. The following theorem provides sufficient conditions for the qth exponential stability of system (1) .

Theorem 2 *Under the same conditions as those considered in Theorem 1, the solution of system (1) with the initial value (2) is qth moment exponentially stable. That is,*

$$\limsup_{t \to \infty} \frac{1}{t} \ln E|x(t)|^q < 0. \tag{27}$$

Proof. Applying (25) yields

$$E\Lambda(t, x(t), \sigma(t)) \leq C_2 e^{-\left(\varepsilon - \frac{\ln \mu_i}{\mathcal{T}_{ai}}\right) t}.$$

Recalling condition (7), we have

$$a_1 E|x(t)|^q \leq C_2 e^{-\left(\varepsilon - \frac{\ln \mu_i}{\mathcal{T}_{ai}}\right) t}. \tag{28}$$

Hence, from (12), we observe that

$$\limsup_{t \to \infty} \frac{1}{t} \ln E|x(t)|^q \leq \limsup_{t \to \infty} \frac{1}{t} \ln C_3 e^{-\left(\varepsilon - \frac{\ln \mu_i}{\mathcal{T}_{ai}}\right) t} = -\left(\varepsilon - \frac{\ln \mu_i}{\mathcal{T}_{ai}}\right) < 0,$$

where $C_3 = \frac{C_2}{a_1}$, which is the required assertion in (27). The proof is completed.

Remark 4 *The difficulty of the proof is that the time delay δ_t is merely a Borel measurable function of t rather than a differentiable function of t[13,28]. This means that the existing results[13,28] cannot be applied to SSS (1). By selecting a suitable form of MLF, the existence and uniqueness of the global solution are initially proven via an inequality scaling technique (i.e., Lemma 1). Subsequently, the L^q-boundedness of the solution is obtained by using the ADT method.*

The following theorem demonstrates that a stronger result can be obtained under proper conditions.

Theorem 3 *Let Assumptions 1-3 hold. If $q > 2\alpha_1 \vee 2\alpha_2$, then the solution of the controlled system (1) with the initial value (2) is almost surely exponentially stable. That is,*

$$\limsup_{t\to\infty} \frac{1}{t} \ln(|x(t)|) < 0 \quad a.s. \tag{29}$$

Proof. Let k be any non-negative integer. Using the Hölder and Doob martingale inequalities[26], we obtain

$$\begin{aligned} E(\sup_{k\le t\le k+1} |x(t)|^2) &\le 4E|x(k+1)|^2 \\ &\le 4[3E|x(k)|^2 + 3E\int_k^{k+1} |f_i(t,x(t),y(t))|^2 dt \\ &+ 12E\int_k^{k+1} |g_i(t,x(t),y(t))|^2 dt]. \end{aligned}$$

From condition (6), we have

$$\begin{aligned} E(\sup_{k\le t\le k+1} |x(t)|^2) \le 12E|x(k)|^2 &+ C_4E\int_k^{k+1} (1+|x(t)|^{2\alpha_1} + |x(t-\delta_t)|^{2\alpha_1})dt \\ &+ C_4E\int_k^{k+1} (1+|x(t)|^{2\alpha_2} + |x(t-\delta_t)|^{2\alpha_2})dt, \end{aligned}$$

where C_4 is a positive constant. According to $q > 2\alpha_1 \vee 2\alpha_2$, we derive

$$E|x(t)|^{2\alpha_1} \le (E|x(t)|^q)^{\frac{2\alpha_1}{q}} \le 1 + E|x(t)|^q.$$

Similarly, we also have

$$E|x(t)|^{2\alpha_2} \le 1 + E|x(t)|^q.$$

From (28), it follows that

$$E\int_k^{k+1} |x(t)|^{2\alpha_1} dt \le 1 + E\int_k^{k+1} |x(t)|^q dt \le 1 + E\int_k^{k+1} C_3 e^{-\hat{\varepsilon}t} dt \le C_5 e^{-\hat{\varepsilon}k},$$

where C_5 is a positive constant, $\hat{\varepsilon} = \varepsilon - \dfrac{ln\mu_i}{\mathcal{J}_{ai}}$. Consequently, we can deduce that

$$E\left(\sup_{k\le t\le k+1} |x(t)|^2\right) \le C_5 e^{-\hat{\varepsilon}k}.$$

By the Doob martingale inequality, it follows that

$$\sum_{k=0}^{\infty} P\left(\sup_{k\le t\le k+1} |x(t)| > e^{-0.25\hat{\varepsilon}k}\right) \le \sum_{k=0}^{\infty} C_5 e^{-0.5\hat{\varepsilon}k} < \infty.$$

From the well-known Borel-Cantelli lemma [4], it follows that for almost all $\omega \in \Omega$, there exists a positive integer $k_0 = k_0(\omega)$ such that

$$\sup_{k \le t \le k+1} |x(t)| \le e^{-0.25\hat{\varepsilon}k}.$$

Therefore, for almost all $\omega \in \Omega$,

$$\frac{1}{t}\ln(|x(t)|) \le -\frac{0.25\hat{\varepsilon}k}{(k+1)}, \quad t \in [k, k+1], \quad k \ge k_0.$$

Then, we can obtain

$$\limsup_{t\to\infty} \frac{1}{t}\ln(|x(t)|) \le -0.25\hat{\varepsilon} < 0 \quad a.s.$$

which is the required assertion in (29). Thus, the proof is completed.
So far, we can conclude that under Assumptions 1-3, system (1) is not only qth moment exponentially stable but also almost surely exponentially stable.

Remark 5 *In general, for a stochastic nonlinear system, the qth moment exponential stability does not imply almost surely exponential stability without any imposed conditions. However, this result can be ensured using the PGC (6). Similar arguments can be found in [4,13].*

Remark 6 *In this paper, the highly nonlinear SSSs with time-varying delays are considered, in which the switching signal is deterministic and differs from those considered in [13,16,29–32]. In the current study on stochastic systems with Markovian switching [13,16,29–32], M matrix theory is an efficient tool for achieving stochastic stability. However, this method is not valid for SSS (1) because a deterministic switching signal rather than the Markovian switching signal is involved in (1). In this paper, a new stability analysis based on the ADT method coupled with the MLF approach is developed for SSSs. In our proof, the Lyapunov functions do not need to be specified initially, which increases the flexibility for the choice of Lyapunov functions in practice.*

4. NUMERICAL EXAMPLE

In this section, a numerical example is presented to validate the derived results. Consider the following highly nonlinear SSS with a time-varying delay:

$$dx(t) = f_{\sigma(t)}(t, x(t), x(t-\delta(t)))dt + g_{\sigma(t)}(t, x(t), x(t-\delta(t)))dB(t), \tag{30}$$

where the time-varying delay $\delta_t = \frac{1}{2} + \frac{1}{4}|\sin(10t)|$, the initial data $x(\theta) = \xi = 0.1\pi$ with $-\frac{3}{4} \le \theta \le 0$, and

$$f_1(t,x,y) = -x - x^3 + \frac{1}{3}y^2, g_1(t,x,y) = \frac{1}{4}y + \frac{1}{4}y^2,$$
$$f_2(t,x,y) = -x + \frac{1}{3}y - \frac{4}{3}x^3 + \frac{1}{3}y^2, g_2(t,x,y) = \frac{1}{4}y^2.$$

In addition, we set $\Lambda(t,x,1) = x^6$ and $\Lambda(t,x,2) = \frac{11}{12}x^6$. It is not difficult to verify that Assumption 1 holds with $m_1 = \frac{1}{2}$, $m = \frac{3}{4}$, and $\bar{m} = \frac{4}{3}$, and f_1, f_2, g_1, g_2 satisfy Assumption 2. Then, we have $a_1 = \frac{11}{12}$, $a_2 = 1$ and $\mu_1 = \mu_2 = \frac{11}{10}$, which satisfy (7) and (8). A direct computation yields

$$\begin{aligned}\mathcal{L}\Lambda(t,x,y,1) &= 6x^5(-x - x^3 + \frac{1}{3}y^2) + \frac{30}{2}x^4(\frac{1}{4}y + \frac{1}{4}y^2)^2 \\ &\le -\frac{407}{112}x^8 + \frac{169}{112}y^8 - \frac{93}{28}x^6 + \frac{67}{56}y^6.\end{aligned}$$

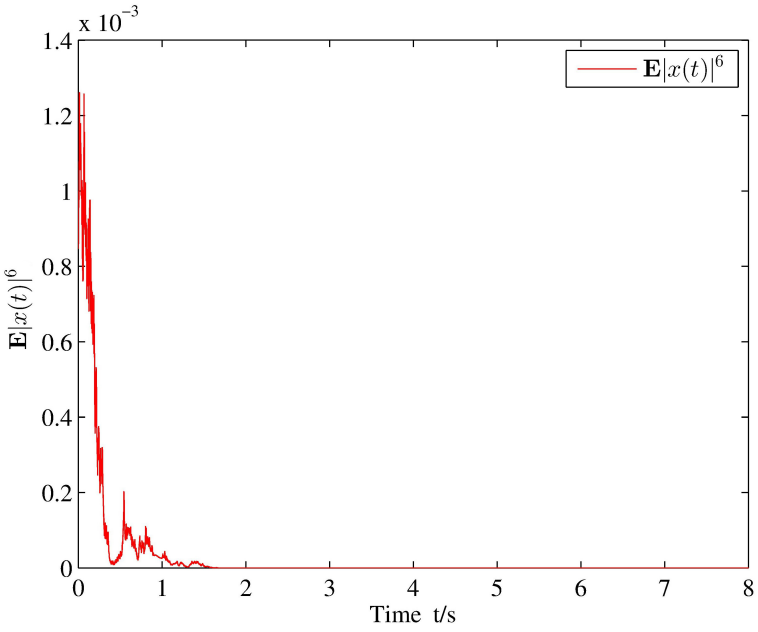

Figure 2. The exponential stability in L^6 of system (30).

and

$$\begin{aligned}\mathcal{L}\Lambda(t,x,y,2) =& \frac{11}{2}x^5(-x+\frac{1}{3}y-\frac{4}{3}x^3+\frac{1}{3}y^2)+\frac{55}{4}x^4(\frac{1}{4}y^2)^2\\ \leq& -\frac{15037}{2688}x^8+\frac{2563}{2688}y^8-\frac{671}{252}x^6+\frac{209}{252}y^6.\end{aligned}$$

Then, we obtain

$$\mathcal{L}\Lambda(t,x,y,i) \leq -\frac{407}{112}x^8+\frac{169}{112}y^8-\frac{671}{252}x^6+\frac{67}{56}y^6,$$

which means that the condition (9) holds with $\lambda_1 = -\frac{407}{112}, \lambda_2 = \frac{169}{112}, \lambda_3 = \frac{671}{252}, \lambda_4 = \frac{67}{56}, W(x) = |x|^8, W(y) = |y|^8$, and $q = 6$. Let $\mathcal{T}_{a1} = \mathcal{T}_{a2} = 1s$ (i.e., the active period of each subsystem is 1 s) and $N_{01} = N_{02} = 0.1$. From (11) and (12), we can compute that the constant ε should satisfy $0.0953 < \varepsilon < 0.7883$. Then, it follows from (10) that $\varepsilon = 0.4414$. According to Theorem 1, the highly nonlinear SSS (30) has a unique global solution on $[-\frac{3}{4}, \infty)$ and is bounded. In addition, the system (30) is not only 6th moment exponentially stable but also almost surely exponentially stable. Figure 2 shows that the system (30) is exponentially stable in 6th moment. Figure 3 shows that the system (30) is exponentially stable in the sample path. Figure 4 shows the switching signal $\sigma(t)$.

5. CONCLUSIONS

In this paper, the existence of a unique global solution for a highly nonlinear SSS with a deterministic switching signal is examined by using the ADT method coupled with the MLF approach. The stability criteria of qth moment exponential stability and almost surely exponential stability of the highly nonlinear SSS are stated. Finally, a numerical example is presented to illustrate the effectiveness of the obtained results. Inspired by recent studies[7,20,33–36], two further research directions have emerged: (1) Solving the problem of stability for highly nonlinear SSSs with impulsive effects under asynchronous switching, and (2) designing a control input function to stabilize a highly nonlinear SSS with a time-varying delay.

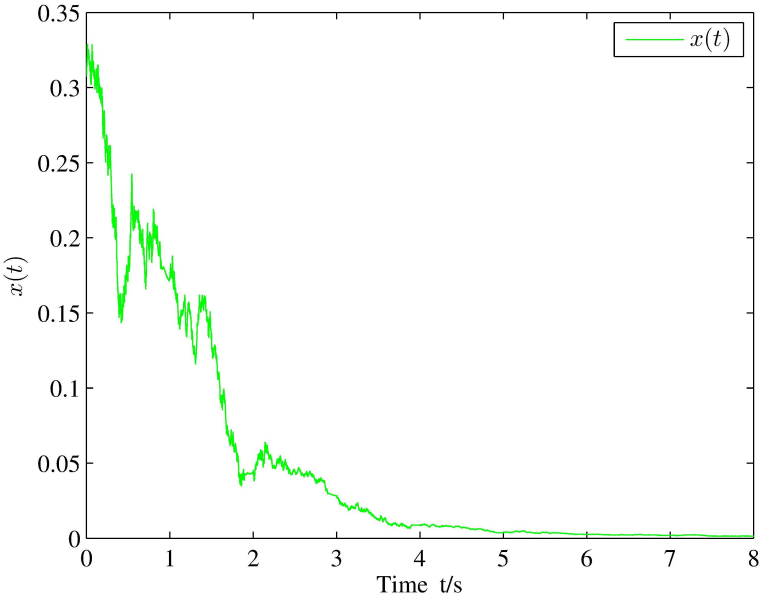

Figure 3. Exponential stability in the sample path of the system (30).

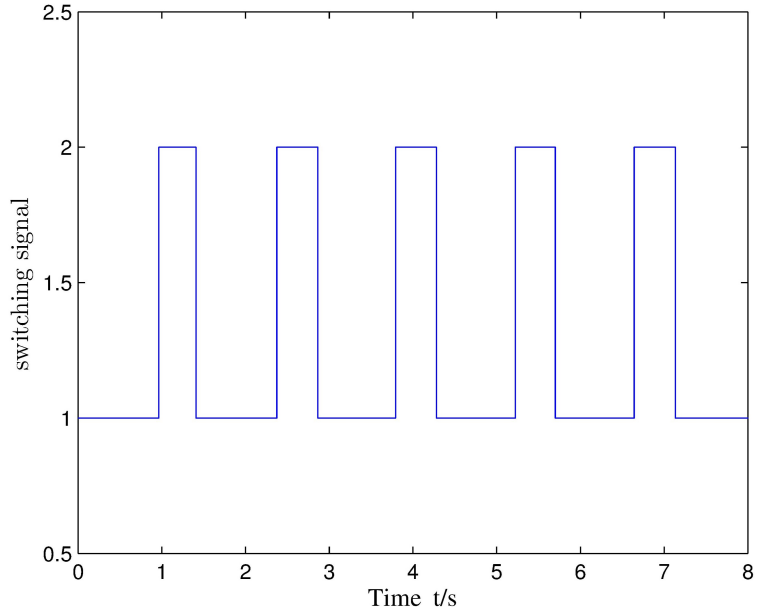

Figure 4. Switching signal $\sigma(t)$.

DECLARATIONS

Authors' contributions

Made substantial contributions to supervision, writing, review, editing and methodology: Wang H
Performed writing-original draft, software, validation and visualization: Sun J

Availability of data and materials

Not applicable.

Financial support and sponsorship
This work was jointly supported by the National Natural Science Foundation of China (62003170), and the Natural Science Foundation of Jiangsu Province (BK20190770).

Conflicts of interest
All authors declared there are no conflicts of interest.

Ethical approval and consent to participate
Not applicable.

Consent for publication
Not applicable.

REFERENCES

1. Zhang R, Quan Q, Cai KY. Attitude control of a quadrotor aircraft subject to a class of time-varying disturbances. *IET Control Theory & Applications* 2011;5:1140-6. DOI
2. Yoshida T, Jones LE, Ellner SP, Fussmann GF, Hairston NG Jr. Rapid evolution drives ecological dynamics in a predator-prey system. *Nature* 2003;424:303-6. DOI
3. Preis T, Schneider JJ, Stanley HE. Switching processes in financial markets. *Proc Natl Acad Sci U S A* 2011;108:7674-8. DOI
4. Mao XR, Yuan CG. Stochastic Differential Equations with Markovian Switching. London: Imperial College Press, 2006.
5. Wu XT, Tang Y, Cao JD. Input-to-state stability of time-varying switched systems with time delay. *IEEE Trans Automat Contr* 2019;64:2537-44. DOI
6. Xiao HN, Zhu QX, Karimi HR. Stability of stochastic delay switched neural networks with all unstable subsystems: a multiple discretized Lyapunov-Krasovskii functionals method. *Inf Sci* 2022;582:302-15. DOI
7. Yuan S, Zhang LX, Schutter BD, Baldi S. A novel Lyapunov function for a non-weighted $\mathcal{L}_2$ gain of asynchronously switched linear systems. *Automatica* 2018;87:310-17. DOI
8. Cheng P, He SP, Luan XL, Liu F. Finite-region asynchronous H_∞ control for 2D Markov jump systems. *Automatica* 2021;129:109590. DOI
9. Wang B, Zhu QX. Stability analysis of Markov switched stochastic differential equations with both stable and unstable subsystems. *Systems & Control Letters* 2017;105:55-61. DOI
10. Liberzon D. Finite data-rate feedback stabilization of switched and hybrid inear systems. *Automatica* 2014;50:409–20. DOI
11. Sun ZD, Ge SS. Stability theory of switched dynamical systems. https://doi.org/10.1007/978-0-85729-256-8 [Last accessed on 22 Dec 2022]
12. Hu LJ, Mao XR, Shen Y. Stability and boundedness of nonlinear hybrid stochastic differential delay equations. *Syst & Contr Let* 2013;62:178–87. DOI
13. Li XY, Mao XR. Stabilisation of highly nonlinear hybrid stochastic differential delay equations by delay feedback control. *Automatica* 2020;112:108657. DOI
14. Zhu QX. Stabilization of stochastic nonlinear delay systems with exogenous disturbances and the event-triggered feedback control. *IEEE Trans Automat Contr* 2019;64:3764-71. DOI
15. Zhu QX, Song SY, Shi P. Effect of noise on the solutions of non-linear delay systems. *IET Control Theory & Appl* 2018;12:1822-9. DOI
16. Dong HL, Mao XR. Advances in stabilization of highly nonlinear hybrid delay systems. *Automatica* 2022;136:110086. DOI
17. Zhao Y, Wu XT, Gao JD. Stability of highly non-linear switched stochastic systems. *IET Control Theory & Applications* 2019;13:1940-44. DOI
18. Liu L, Yin S, Zhang LX, Yin XY, Yan HC. Improved results on asymptotic stabilization for stochastic nonlinear time-delay systems with application to a chemical reactor system. *IEEE Transactions on Sysems, Man, and Cybernetics: Systems* 2016;47:195-204. DOI
19. Hu W, Zhu QX, Karimi HR. Some improved razumikhin stability criteria for impulsive stochastic delay differential systems. *IEEE Trans Automat Contr* 2019;64:5207-13. DOI
20. Yuan S, Zhang LX, Baldi S. Adaptive stabilization of impulsive switched linear time-delay systems: a piecewise dynamic gain approach. *Automatica* 2019;103:322-29. DOI
21. Lian J, Feng Z. Passivity analysis and synthesis for a class of discrete-time switched stochastic systems with time-varying delay. *Asian J Control* 2013;15:501-11. DOI
22. Cong S, Yin LP. Exponential stability conditions for switched linear stochastic systems with time-varying delay. *IET Control Theory & Applications* 2012;6:2453-59. DOI

23. Yue D, Han QL. Delay-dependent exponential stability of stochastic systems with time-varying delay, nonlinearity, and markovian switching. *IEEE Trans Automat Contr* 2005,50:217-22. DOI
24. Zeng HB, Liu XG, Wang W. A generalized free-matrix-based integral inequality for stability analysis of time-varying delay systems. *Applied Mathematics and Computation* 2019;354:1-8. DOI
25. Chen HB, Shi P, Lim CC, Hu P. Exponential stability for neutral stochastic markov systems with time-varying delay and its applications. *IEEE Trans Cybernetics* 2015;46:1350-62. DOI
26. Mao XR. Stochastic differential equations and applications. Elsevier; 2007.
27. Zhao Y, Zhu QX. Stability of highly nonlinear neutral stochastic delay systems with non-random switching signals. *Syst & Contr Let* 2022;165:105261. DOI
28. Zhao Y, Zhu QX. Stabilization by delay feedback control for highly nonlinear switched stochastic systems with time delays. *Int J Robust Nonlinear Control* 2021;31:3070-89. DOI
29. Fei WY, Hu LJ, Mao XR, Shen MX. Structured robust stability and boundedness of nonlinear hybrid delay systems. *SIAM J Control Optim* 2018;56:2662-89. DOI
30. Shen MX, Fei C, Fei WY, Mao XR. Stabilisation by delay feedback control for highly nonlinear neutral stochastic differential equations. *Syst & Contr Let* 2020;137:104645. DOI
31. Shen MX, Fei WY, Mao XR, Deng SN. Exponential stability of highly nonlinear neutral pantograph stochastic differential equations. *Asian J Control* 2020;22:436-48. DOI
32. Song RL, Wang B, Zhu QX. Delay-dependent stability of nonlinear hybrid neutral stochastic differential equations with multiple delays *Int J Robust Nonlinear Control* 2021;31:250-67. DOI
33. Kang Y, Zhai DH, Liu GP, Zhao YB, Zhao P. Stability analysis of a class of hybrid stochastic retarded systems under asynchronous switching. *IEEE Trans on Automat Contr* 2014;59:1511-23. DOI
34. Shen MX, Fei C, Fei WY, Mao XR, Mei CH. Delay-dependent stability of highly nonlinear neutral stochastic functional differential equations. *Intl J Robust & Nonlinear* 2022;32:9957-76. DOI
35. Ren MF, Zhang QC, Zhang JH. An introductory survey of probability density function control. *Syst Sci & Contr Eng* 2019;7:158-70. DOI
36. Zhang QC, Wang H. A novel data-based stochastic distribution control for non-Gaussian stochastic systems. *IEEE Trans Automat Contr* 2021;67:1506-13. DOI

Bao *et al. Complex Eng Syst* 2022;2:16
DOI: 10.20517/ces.2022.30

Complex Engineering Systems

Research Article

Open Access

Pulsar identification based on generative adversarial network and residual network

Zelun Bao, Guiru Liu, Yefan Li, Yanxi Xie, Yang Xu, Zifeng Zhang, Qian Yin, Xin Zheng

School of Artificial Intelligence, Beijing Normal University, Beijing 100875, China.

Correspondence to: Dr. Qian Yin, School of Artificial Intelligence, Beijing Normal University, No.19 Xinwai Street, Beijing 100875, China. E-mail: yinqian@bnu.edu.cn; ORCID: 0000-0002-0354-5490

How to cite this article: Bao Z, Liu G, Li Y, Xie Y, Xu Y, Zhang Z, Yin Q, Zheng X. Pulsar identification based on generative adversarial network and residual network. *Complex Eng Syst* 2022;2:16. http://dx.doi.org/10.20517/ces.2022.30

Received: 14 Sep 2022 **First Decision:** 21 Oct 2022 **Revised:** 19 Nov 2022 **Accepted:** 28 Nov 2022 **Published:** 8 Dec 2022

Academic Editor: Hamid Reza Karimi **Copy Editor:** Fanglin Lan **Production Editor:** Fanglin Lan

Abstract

The search for pulsars is an important area of study in modern astronomy. The amount of collected pulsar data is increasing exponentially as the performance of modern radio telescopes improves, necessitating the improvement of the original pulsar search methods. Artificial intelligence techniques are currently being used in pulsar candidate identification tasks. However, improving the accuracy of pulsar candidate identification using artificial intelligence techniques remains a challenge. Because the amount of collected data is so large, the number of real pulsar samples is very limited, which leads to a serious sample imbalance problem. Many existing methods ignore this issue, making it difficult for the model to reach the optimal solution. A framework combining generative adversarial networks and residual networks is proposed to greatly alleviate the problem of sample inequality. The framework first generates stable pulsar images using generative adversarial networks and then designs a deep neural network model based on residual networks to identify pulsar candidates using intra-block and inter-block residual connectivity. The ResNet approach has a better ability to fit the data than the CNN approach and can achieve the extraction of features with more classification ability with a smaller dataset. Meanwhile, the data expanded by the high-quality simulated samples generated by the generative adversarial network can provide richer identification features and improve the identification accuracy for pulsar candidates.

Keywords: Pulsar, candidate recognition, artificial intelligence, generative adversarial network, residual network

1. INTRODUCTION

The search for pulsars is of great importance in the study of astronomy, physics and other fields, including gravitational waves, state equations of dense substances, stellar evolution, dark matter and dark energy, and the formation and evolution of binary and multiple star systems. Therefore, the discovery of new pulsars and the exploration of their substantial scientific research potential are of great value and importance.

At present, more than 2,700 pulsars have been discovered in the whole galaxy[1]. Most of the pulsars were discovered by modern radio telescopes, which receive periodic radio signals, pre-process them and package them into the data we need. The generation of pulsar candidates from the collected data is basically divided into three procedures which are eliminating RFI, de-dispersion, and fast fourier transform (FFT)[2]. This strategy is generally how the samples of pulsar candidates are generated. With the continuous improvement of modern radio telescopes, samples of pulsar candidates have increased, but only a small fraction of these samples are real pulsars due to the presence of RF interference and different noise sources. As a result, the real sample of pulsar candidates is much smaller than the non-real sample. In traditional studies, manual experts review each candidate in 1-300 s[3], and it takes more than 70,000 h to examine millions of pulsar candidates. Therefore, it is crucial to investigate an automatic, efficient and accurate method for pulsar candidate identification.

In recent years, a large number of object detection methods based on neural networks have been proposed[4], many of which have been selected for pulsar candidate detection. Pulsar candidate identification methods based on neural networks have been proposed to handle the huge amount of pulsar data. Bates *et al.*[5] used artificial neural networks to automatically identify plausible pulsar candidates from pulsar measurements. Morello *et al.*[6] proposed a method called SPINN (Straightforward Pulsar Identification using Neural Networks), which designed a pulsar candidate classifier that tended to maximize the recall of identification. Zhu *et al.*[7] developed a pulsar image-based classification system (PICS) that used image pattern recognition and deep neural networks to identify pulsars in recent measurements, and Lyon *et al.*[8] proposed the decision tree-based recognition model Very Fast Decision Tree (VFDT), a method that found 20 new pulsars using the LOTAAS dataset.

Although the above neural network-based methods have achieved good identification results on the corresponding datasets and helped astronomers discover new pulsars, there are still some problems. Among the currently available pulsar candidate data, the number of positive samples (real pulsars) among the labelled pulsar candidates is extremely limited, and the number of negative samples (non-real pulsars) is much higher than the number of positive samples. In this case, when some deep learning models are directly used for training, the imbalance between the number of positive and negative samples leads to poor classification, overfitting, and even possible training failure. To address this issue, Lyon *et al.*[9] confirmed that the imbalance problem of pulsar candidate samples reduces the recall of pulsars by executing different classifiers on the HTRU dataset[10]. Then Lyon *et al.*[11] proposed using the Hellinger distance (HDT) as a splitting criterion for VFDT, thus alleviating the sample imbalance problem. In addition, GAN methods have recently been widely used in pulsar candidate identification[12]. For example, Guo *et al.*[13] proposed using Generative Adversarial Networks (GAN)[14] to generate some positive pulsar sample data to alleviate the problem of low recall for pulsar candidate identification models on unbalanced datasets.

Although the above methods can alleviate the sample imbalance problem to a certain extent, the traditional GAN model suffers from the pattern collapse problem while generating positive samples[15]. Therefore, WGAN[16], a Wasserstein distance-based generative adversarial network, is recommended in the proposed method to alleviate the pattern collapse problem and enlarge the present pulsar dataset. WGAN was first utilized to generate some images that approximate the real pulsar as positive samples and then fuse the generated positive sample images into an unbalanced dataset to train the pulsar recognition model. Experiments proved that training the deep neural network model on the balanced dataset could further improve the model's recog-

nition accuracy. In addition, since the residual network[17–19] is able to overcome the gradient disappearance problem in the deep neural network model, a deep neural network model containing intra-block residual connections and inter-block residual connections was included in the proposed model during the pulsar candidate identification stage. Experiments proved that the module achieved optimal recognition accuracy in all scenarios compared to the shallow deep neural network model.

In this paper, two basic methods utilized in the proposed model are first introduced with detailed figures and illustrations. These basic methods are the generative adversarial network-based pulsar image generation method and the residual network-based pulsar candidate identification method. Then, the HTRU-Medlat dataset is used in the proposed model and the experimental results are obtained; these results indicate that the proposed model achieves the best performance in the experiment without any other complicated data generation method, which is why HTRU-Medlat was chosen as the dataset for the experiment. In the proposed model, a time-versus-phase plot and a frequency-versus-phase plot are used to implement the screening of pulsar candidates and describe their characteristics of pulsar candidates so that samples can be better evaluated. As a result, positive samples can be identified more accurately, which is essential because positive samples represent the essential information of pulsar candidates. After collecting the experimental results, several evaluation indicators, including Precision, Recall and F1-score, are selected to assess our experimental results. Finally, the results of the proposed models are compared with other existing models. The experimental results show that ResNet exhibits a better ability to fit data and extract features on small datasets and large datasets containing images generated by generative adversarial networks compared to CNN methods. In the comparison experiments between the small dataset and the extended large dataset, the improved F1 values and accuracy metrics of the CNN method indicate that the simulated sample-extended data generated by the generative adversarial network can improve the model's accuracy to some extent. Through experimental validation, better results are obtained: the quality of the large dataset extended with simulated samples is improved, providing richer recognition features, and the recognition accuracy is further improved[4].

2. METHODS

In this paper, a framework combining generative adversarial networks and residual networks is proposed for pulsar candidate identification. First, the generative adversarial networks module is used to tackle the imbalance problem in the dataset, and it is able to generate a series of pulsar candidate images that approximate positive samples to expand the existing pulsar dataset. Then, based on the idea of residual connectivity, this paper designs a deep neural network for pulsar candidate identification utilizing intra- and inter-block residual connectivity, which can effectively improve the recognition accuracy.

2.1. Generative adversarial network-based pulsar image generation method

In this paper, the Wasserstein distance[19] is used to replace the Jensen-Shannon (JS) divergence of the traditional GAN[20,21] because it can more explicitly measure the difference between two different distributions. Wasserstein GAN (WGAN) based on the Wasserstein distance can overcome problems such as the gradient vanishing and mode collapse experienced by the traditional GAN training, and it can generate more stable pulsar images.

The architecture of the generator is illustrated in Figure 1. The generator produces $1 \times 48 \times 48$ grey images by accepting 1×1024-dimensional Gaussian noise as inputs. First, the Gaussian noise is transformed into a 1×18432 tensor with a 1024×18432 fully connected layer. Then, it is projected and reshaped into a $128 \times 12 \times 12$ tensor with 128 channels. In the next two convolutions, kernels of size 4×4 are adopted and the numbers of channels are 64 and 1. The LeakyReLU activation function with a slope of 0.1 is used for all of the convolutions except the last one, and the sigmoid activation function is used in the last convolutional layer to ensure that the pixel values of the final output are in the range $[0, 1]$ to generate appropriate grey images.

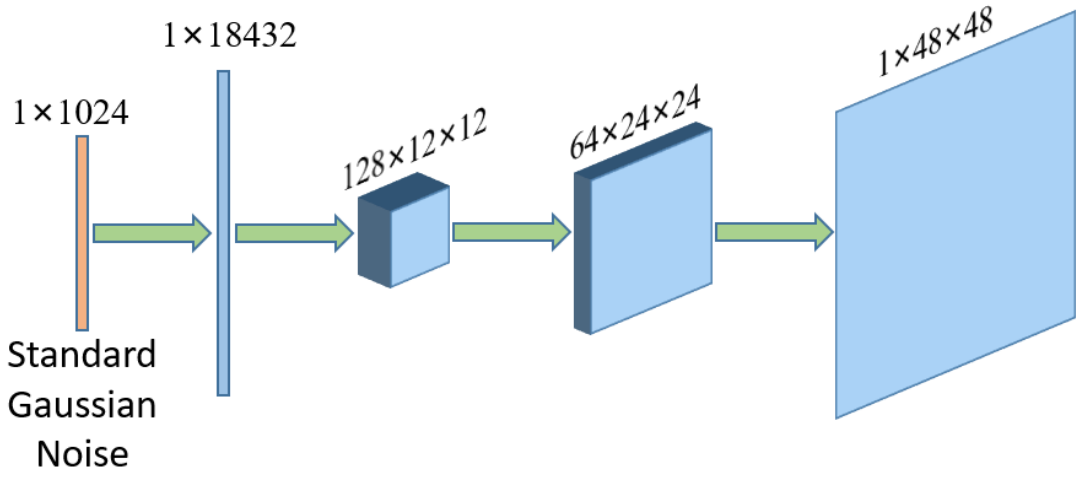

Figure 1. Generator architecture. The input is 1 × 1024-dimensional Gaussian noise; that input is first transformed into a 1 × 18432 tensor with a 1024 × 18432 fully connected layer. Then the tensor is projected and reshaped into a 128 × 12 × 12 tensor. There are two convolution layers. The output is a generated 1 × 48 × 48-dimensional grey image.

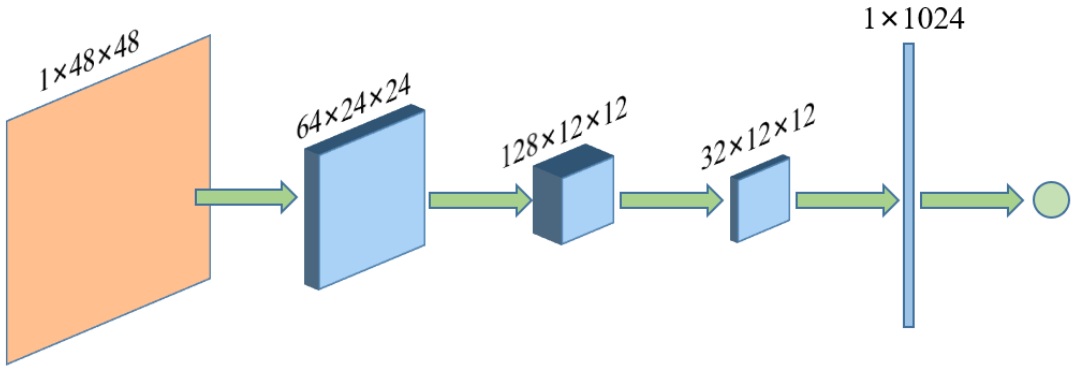

Figure 2. Discriminator architecture. The input samples are 1 × 48 × 48 grey images, and here are three convolution layers. After the convolution, the images are reshaped into 1 × 1024-dimensional tensors.

The structure of the discriminator is illustrated in Figure 2. The discriminator designed in this paper accepts 1 × 48 × 48-dimensional grey images as inputs and then obtains the scoring of the corresponding image and calculates the Wasserstein distance between the real data and the simulated data. The first two convolutions use a 4 × 4 convolution kernel, and the last convolution uses a 3 × 3 convolution kernel. There are 64, 128 and 32 channels for these three convolutional layers. After the convolution, the image is reshaped into a two-dimensional tensor, and the image score is calculated with a fully connected layer. The LeakyReLU activation function with a slope of 0.1 is used for all layers except the last fully connected layer. However, the sigmoid activation function is not used in the last layer because the Wasserstein distance is used instead of the original JS distance. It is empirically shown [16] that this model can significantly alleviate the mode collapse problem of the generative adversarial network.

The generator and discriminator are trained iteratively throughout the training process. The Wasserstein distance between the simulated pulsar sample and the real pulsar sample is optimised iteratively, and the simulated pulsar sample produced by the generator is finally able to accurately characterize the real sample.

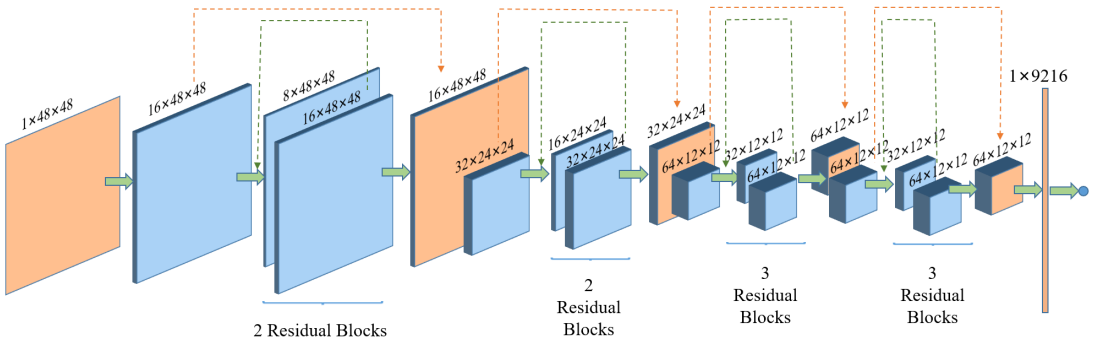

Figure 3. An illustration of the pulsar identification model. The blue colour indicates the convolution process, and the orange colour indicates the hidden state. The green dashed line indicates the intra-module residual connections, and the red dashed line indicates the inter-module residual connections. The inputs are the 1 × 48 × 48 grey images. There are four modules, and the outputs are 1 × 9216 features.

Table 1. Confusion matrix of the dichotomous problem

	Predicted class: Negative (N)	Predicted class: Positive (P)
Actual class: True (T)	TN	TP
Actual class: False (F)	FN	FP

2.2. Residual network-based pulsar candidate identification method

In this paper, a residual network with 24 CNN layers [Figure 3] is designed for pulsar candidate identification. Unlike the original residual network, the proposed residual network has both intra-module residual connections (Figure 3, green dashed line) and inter-module residual connections (Figure 3, red dashed line). The blue colour indicates the convolution process and the orange colour indicates the hidden state. There are four modules in the convolution process, each of which has a stacking number of 2, 2, 3, and 3 layers. A pulsar candidate image of size 1×48×48 is first generated as a 16 × 48 × 48 tensor by the first convolutional layer, which has a convolution kernel size of 3 × 3 and a channel number of 16. The image is then input into the first module; this module first reduces the number of channels to 8, which is then raised to 16 to output a 16×48×48 tensor. That tensor is then input into the same module again with non-shared parameters. At the end of the first module, the final output is added to the input tensor of the same dimension before the first module to obtain a 16 × 48 × 48 orange tensor as the input to the next module [Figure 3]. Therefore, repeatedly, after four modules that employ the convolution operation, the final output feature map is a 1 × 9216 tensor, which is used for future identifications.

3. RESULTS

3.1. Datasets and evaluation indicators

The pulsar candidate dataset used for the experiments is HTRU-Medlat, which is first publicly available labelled pulsar dataset published by Morello *et al*[6]. The dataset is a collection of labelled pulsar candidates from the intermediate galactic latitude part of the HTRU survey, and it contains exactly 1,196 positive samples from 521 distinct sources and 89,996 negative candidates. In addition, the HTRU-Medlat dataset contains both temporal phase (ints) images and frequency phase (bands) images. The evaluation indicators used in the pulsar candidate identification problem are: Precision, Recall and F1-score. Table 1 shows the confusion matrix for the binary classification problem, which classifies all possible predictions in that problem.

The assessment indicators used in this paper can be obtained by using a dichotomous confusion matrix.

(1) Accuracy rate: the proportion of samples with positive predictions that are correctly predicted, i.e.,:

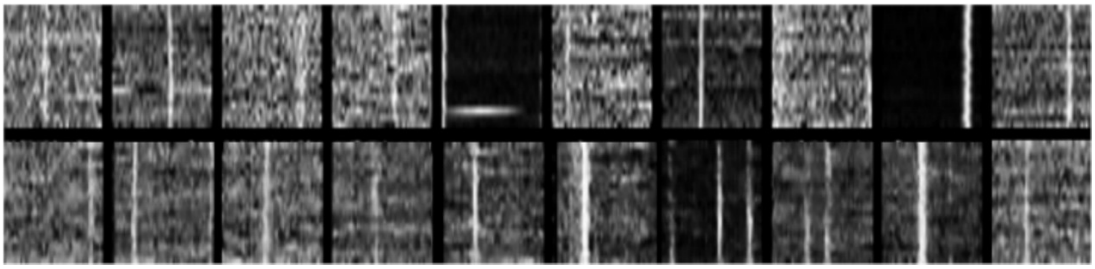

Figure 4. Simulation samples generated based on the generative adoration network (time-phase images of the HTRU-Medlat dataset).

$$Precision = \frac{TP}{TP + FP} \tag{1}$$

(2) Recall: the proportion of all samples with positive true labels that are correctly predicted to be positive, i.e.,:

$$Recall = \frac{TP}{TP + FN} \tag{2}$$

(3) F1-score: the combined accuracy and recall is the F1-score, i.e.,:

$$F1 - score = \frac{2 \times Precision \times Recall}{Precision + Recall} \tag{3}$$

3.2. Model comparison experiment

The proposed model uses a CNN [7] model for comparison, which has a similar structure to the LeNet network structure [22], but with some adaptations for the pulsar candidate identification task. For the hyperparameter settings of the residual network model, this paper uses a mini-batch size of 128, a learning rate of 0.001, a size of 0.00001 for the L2 regularisation term, and a standard Gaussian to initialise the model parameters. In addition, the model employs the ReLU [23] activation function for all layers except the last layer of the model, which uses a sigmoid activation function. The objective function for optimisation is cross-entropy, and the Adam [24] optimiser is used.

For the generative adversarial network's hyperparameter settings, the learning rate is 0.001, the L2 regularization weight is 0.0005, the number of training rounds is 200, the optimiser is Adam, the size of the minibatch is 128, the parameters are initialized using Kaiming initialization [25], the discriminator is trained with 5 rounds for each batch, the discriminator weights range from [-0.005, 0.005], and LeakyReLU employed a slope of 0.1.

The simulated positive samples generated by the trained generator in this paper are shown in Figure 4, where the ten images in the first row are the real pulsar samples and the ten images in the second row are the simulated samples produced by the generator in this paper. It can be seen that the simulated samples generated by the model can retain the features of the real pulsar samples to a certain extent.The training loss on the HTRU-Medlat dataset is demonstrated in Figure 5, which reveals the optimised training performance of the proposed method in the experiment. The training loss curve declines sharply when the quantity of training samples is relatively small, and the simulated and real pulsar image loss remains fairly low at 4% when the dataset is expanded. The training loss of the proposed method is significantly lower than that of other existing models, thus guaranteeing better performance in pulsar sample identification.

Figure 5. Training loss curve on the HTRU-Medlat dataset.

Table 2. HTRU-Medlat dataset partitioning after expansion

Sample size	of real samples	of fake samples
Total number of samples in the original dataset	1,196	89,996
IDS training set size	696	10,000
BDS training set size	10,000	10,000
Test set size	500	500

To verify that the generative model can alleviate the problem of sample imbalance, we divide the dataset into two cases, one is an imbalanced data scenario (IDS) with 696 real samples and 10,000 fake samples, and the other is a balanced data scenario (BDS) with 10,000 real samples and 10,000 fake samples. For the HTRU-Medlat dataset, the detailed partitioning scenarios are shown in Table 2.

This paper uses a CNN [7] model for comparison, which has a similar structure to the LeNet network structure [22], but with some adaptations for the pulsar candidate identification task. For the hyperparameter settings of the residual network model, this paper uses a mini-batch size of 128, a learning rate of 0.001, and a size of 0.00001 for the L2 regularisation term used. We also used a standard Gaussian to initialise the parameters of the model and a ReLU [23] activation function for all layers except the last layer of the model, which uses a sigmoid activation function. The objective function for optimisation is cross-entropy, and the Adam [24] optimiser is used.

For the hyperparameter settings of the generative adversarial network, the learning rate is 0.001, the L2 regularization weight is 0.0005, the number of training rounds is 200, the optimizer is Adam, the size of the minibatch is 128, the parameters are initialized using Kaiming initialization [25], the discriminator is trained with 5 rounds for each batch, the discriminator weights range from [-0.005, 0.005], and LeakyReLU employed a slope of 0.1.

The simulated samples are generated using the generative model based on the generative adversarial networks designed in this paper. During the training process, real samples from the IDS training set are used for training. The trained model is then used to generate a series of simulated samples that are used to augment the real sample data. In addition, the simulated samples are filtered, i.e., the generated simulated samples need to be identified as positive by the corresponding residual network model proposed in this paper. The filtered simulated samples are used to expand the IDS training set to obtain the BDS training set.

The results of the automatic identification of pulsar candidates for each method on the HTRU-Medlat dataset are shown in Table 3. "Subints" indicates that the temporal phase images were input, and "Subbands" indicates that the frequency phase images were input. The method with "IDS" indicates that the experiment was tested with small data, while "BDS" indicates that a large dataset consisting of images generated by a generative adversarial network was incorporated. In the IDS data set scenario, the F1 value of the CNN model method reached approximately 95%, while the F1 value of the ResNet method proposed in this paper reached 97.3%

Table 3. Results of GAN-based generated images on the HTRU-Medlat dataset

Model & Dataset	F1-score	Recall	Precision
CNN			
Subints (IDS)	95.6%	94.8%	96.3%
Subints (BDS)	96.9%	94.0%	99.9%
Subbands (IDS)	95.8%	95.4%	96.2%
Subbands (BDS)	97.3%	94.8%	99.9%
ResNet			
Subints (IDS)	97.3%	96.4%	98.3%
Subints (BDS)	98.2%	98.0%	98.4%
Subbands (IDS)	97.5%	95.7%	99.3%
Subbands (BDS)	98.3%	97.4%	99.3%

Table 4. Comparison of the effects of different pulsar candidate identification methods

Model	Literature	Disadvantage/Advantage
Traditional	Eatough RP, Molkenthin N, Kramer M, Noutsos A, Keith M, et al. Selection of radio pulsar candidates using artificial neural networks. Monthly Notices of the Royal Astronomical Society 2010;407:2443–50. [DOI: 10.1111/j.1365-2966.2010.17082.x]	Time-consuming
ANN/CNN	Bates S, Bailes M, Barsdell B, Bhat N, Burgay M, et al. The high time resolution universe pulsar survey—VI. An artificial neural network and timing of 75 pulsars. Monthly Notices of the Royal Astronomical Society 2012;427:1052–65. [DOI: 10.1111/j.1365-2966.2012.22042.x] Morello V, Barr E, Bailes M, Flynn C, Keane E, et al. SPINN: a straightforward machine learning solution to the pulsar candidate selection problem. Monthly Notices of the Royal Astronomical Society 2014;443:1651–62. [DOI: 10.1093/mnras/stu1188] Zhu W, Berndsen A, Madsen E, Tan M, Stairs I, et al. Searching for pulsars using image pattern recognition. The Astrophysical Journal 2014;781:117. [DOI: 10.1088/0004-637x/781/2/117] Lyon RJ, Stappers B, Cooper S, Brooke JM, Knowles JD. Fifty years of pulsar candidate selection: from simple filters to a new principled real-time classification approach. Monthly Notices of the Royal Astronomical Society 2016;459:1104–23. [DOI: 10.1093/mnras/stw656]	Sample imbalance, poor classification
GAN	Guo P, Duan F, Wang P, Yao Y, Yin Q, et al. Pulsar candidate classification using generative adversary networks. Monthly Notices of the Royal Astronomical Society 2019;490:5424–39. [DOI: 10.1093/mnras/stz2975]	Pattern collapse
The proposed model		Alleviates sample imbalance problem, improves the accuracy of recognition

and 97.5% in the ints and bands scenarios respectively, which indicates that the ResNet method is able to fit the data better than the CNN method , and can extract features with more classification ability on a smaller dataset. In addition, when using the BDS method, both models incorporate the simulated samples generated by the generative adversarial network. It can be seen that for the ints and bands images, the CNN method improves the F1 value by 1.3% and 1.5% on the BDS scenarios compared to the IDS scenarios, and the precision metric improves by 3.6% and 3.7% compared to the IDS scenario. In addition, it can be seen that for the ints and bands images, the ResNet method improves Recall by 1.6% and 1.7% for the BDS scenario compared to the IDS scenario, and the F1 values improve by 0.9% and 0.8% compared to the IDS scenario. These results indicate that the data expanded by the simulated samples generated by the generative adversarial network are of higher quality and can provide richer recognition features, which causes the model's recognition to be more accurate to a certain extent.

Different pulsar candidate identification methods are contrasted respectively, as shown in Table 4. For the traditional methods, manual experts review the pulsar candidates slowly, and thus, the models are evidently time-consuming. Neural network-based methods have better identification results but suffer from the sample imbalance problem. The traditional GAN model alleviates the sample imbalance problem to a certain extent but suffers from the pattern collapse problem in the process of generating positive samples. Compared with the previous methods, the proposed method alleviates the sample imbalance and pattern collapse problems, and has a faster identification speed and higher identification accuracy.

4. CONCLUSIONS

In this paper, a generative adversarial network-based pulsar positive sample generation method is proposed for high-quality sample generation in light of the sample imbalance problem in pulsar candidate identification tasks. Training is performed on a dataset containing only positive samples, and the converged model is used to generate a series of high-quality samples to expand the dataset. A residual network-based pulsar candidate identification method is proposed, and it has a better fitting ability compared to shallow neural network models. Comparison experiments have been conducted with recent pulsar identification methods on the HTRU dataset[26], and the experimental results demonstrated that the proposed method achieved optimal results on the dataset compared to the CNN method.

DECLARATIONS

Authors' contributions

Made significant contributions to the conception and experiments: Yin Q, Liu G, Zhe X
Made significant contributions to the writing: Bao Z, Li Y
Made substantial contributions to the revision and translation: Xie Y, Xu Y, Zhang Z

Availability of data and materials

The data underlying this article are available at http://astronomy.swin.edu.au/~vmorello.

Financial support and sponsorship

The research work described in this paper was supported by the Joint Research Fund in Astronomy (U2031136) under cooperative agreement between the NSFC and CAS and the National Key Research and Development Program of China (No. 2018AAA0100203).

Conflicts of interest

All authors declared that there are no conflicts of interest.

Ethical approval and consent to participate

Not applicable.

Consent for publication

Not applicable.

REFERENCES

1. Personalname=Teoh A. The ATNF Pulsar Database. Available from http://astronomy.swin.edu.au/~vmorello/
2. Keith MJ, Jameson A, Van Straten W, et al. The High Time Resolution Universe Pulsar Survey - I. System configuration and initial discoveries. *Monthly Notices of the Royal Astronomical Society* 2010;409:619-27. DOI
3. Eatough RP, Molkenthin N, Kramer M, et al. Selection of radio pulsar candidates using artificial neural networks. *Monthly Notices of the Royal Astronomical Society* 2010;407:2443–50. DOI
4. Shamsolmoali P, Chanussot J, Zareapoor M, Zhou H, Yang J. Multipatch feature pyramid network for weakly supervised object detection in optical remote sensing images. *IEEE Trans Geosci Remote Sensing* 2022;60:1-13. DOI
5. Bates S, Bailes M, Barsdell B, et al. The high time resolution universe pulsar survey—VI. An artificial neural network and timing of 75 pulsars. *Monthly Notices of the Royal Astronomical Society* 2012;427:1052–65. DOI
6. Morello V, Barr E, Bailes M, et al. SPINN: a straightforward machine learning solution to the pulsar candidate selection problem. *Monthly Notices of the Royal Astronomical Society* 2014;443:1651–62. DOI
7. Zhu W, Berndsen A, Madsen E, et al. Searching for pulsars using image pattern recognition. *ApJ* 2014;781:117. DOI

8. Lyon RJ, Stappers B, Cooper S, Brooke JM, Knowles JD. Fifty years of pulsar candidate selection: from simple filters to a new principled real-time classification approach. *Monthly Notices of the Royal Astronomical Society* 2016;459:1104–23. DOI
9. Lyon RJ, Brooke J, Knowles JD, Stappers BW. A study on classification in imbalanced and partially-labelled data streams. In: 2013 IEEE International Conference on Systems, Man, and Cybernetics. IEEE; 2013. pp. 1506–11. DOI
10. Hewish A, Bell SJ, Pilkington JD, Scott PF, Collins RA. 74. Observation of a Rapidly Pulsating Radio Source. In: A Source Book in Astronomy and Astrophysics, 1900–1975. Boston: Harvard University Press; 2013. pp. 498–504. DOI
11. Lyon RJ, Brooke J, Knowles JD, Stappers BW. Hellinger distance trees for imbalanced streams. In: 2014 22nd International Conference on Pattern Recognition. IEEE; 2014. pp. 1969–74. DOI
12. Shamsolmoali P, Zareapoor M, Granger E, et al. Image synthesis with adversarial networks: a comprehensive survey and case studies. *Inform Fusion* 2021;72:126–46. DOI
13. Guo P, Duan F, Wang P, et al. Pulsar candidate classification using generative adversary networks. *Monthly Notices of the Royal Astronomical Society* 2019;490:5424–39. DOI
14. Radford A, Metz L, Chintala S. Unsupervised representation learning with deep convolutional generative adversarial networks. arXiv preprint arXiv:151106434 2015.
15. Zhang CJ, Shang ZH, Chen WM, Xie L, Miao XH. A review of research on pulsar candidate recognition based on machine learning. *Pro Compu Sci* 2020;166:534–38. DOI
16. Arjovsky M, Chintala S, Bottou L. Wasserstein generative adversarial networks. In: International conference on machine learning. PMLR; 2017. pp. 214–23.
17. He K, Zhang X, Ren S, Sun J. Deep residual learning for image recognition. In: Proceedings of the IEEE conference on computer vision and pattern recognition; 2016. pp. 770–78. DOI
18. He K, Zhang X, Ren S, Sun J. Identity mappings in deep residual networks. In: European conference on computer vision. Berlin: Springer; 2016. pp. 630–45. DOI
19. Bousquet O, Gelly S, Tolstikhin I, Simon-Gabriel CJ, Schoelkopf B. From optimal transport to generative modeling: the VEGAN cookbook. arXiv preprint arXiv:170507642 2017. DOI
20. Goodfellow I, Pouget-abadie J, Mirza M, et al. Generative adversarial networks. *Commun ACM* 2020;63:139-44. DOI
21. Radford A, Metz L, Chintala S. Unsupervised representation learning with deep convolutional generative adversarial networks. Computer ence 2015. DOI
22. LeCun Y, Boser B, Denker JS, et al. Backpropagation applied to handwritten zip code recognition. *Neural Computation* 1989;1:541–51. DOI
23. Lecun Y, Bengio Y, Hinton G. Deep learning. *Nature* 2015;521:436. DOI
24. Kingma DP, Ba J. Adam: a method for stochastic optimization. arXiv preprint arXiv:14126980 2014. DOI
25. He K, Zhang X, Ren S, Sun J. Delving deep into rectifiers: Surpassing human-level performance on imagenet classification. In: Proceedings of the IEEE International Conference on Computer Vision; 2015. pp. 1026–34. DOI
26. Naoyuki Y, Keitaro T, Hiroki K, et al. Artificial neural networks for selection of pulsar candidates from radio continuum surveys. *Monthly Notices of the Royal Astronomical Society* 2020;494:1035–44. DOI

AUTHOR INSTRUCTIONS

1. Submission Overview

Before you decide to publish with *Complex Engineering Systems* (*CES*), please read the following items carefully and make sure that you are well aware of Editorial Policies and the following requirements.

1.1 Topic Suitability

The topic of the manuscript must fit the scope of the journal. Please refer to Aims and Scope for more information.

1.2 Open Access and Copyright

The journal adopts Gold Open Access publishing model and distributes content under the Creative Commons Attribution 4.0 International License. Copyright is retained by authors. Please make sure that you are well aware of these policies.

1.3 Publication Fees

CES is an open access journal. When a paper is accepted for publication, authors are required to pay Article Processing Charges (APCs) to cover its editorial and production costs. The APC for each submission is $600. There are no additional charges based on color, length, figures, or other elements. For more details, please refer to OAE Publication Fees.

1.4 Language Editing

All submissions are required to be presented clearly and cohesively in good English. Authors whose first language is not English are advised to have their manuscripts checked or edited by a native English speaker before submission to ensure the high quality of expression. A well-organized manuscript in good English would make the peer review even the whole editorial handling more smoothly and efficiently.

If needed, authors are recommended to consider the language editing services provided by Charlesworth to ensure that the manuscript is written in correct scientific English before submission. Authors who publish with OAE journals enjoy a special discount for the services of Charlesworth via the following two ways.
Submit your manuscripts directly at http://www.charlesworthauthorservices.com/~OAE;
Open the link http://www.charlesworthauthorservices.com/, and enter Promotion Code “OAE” when you

1.5 Work Funded by the National Institutes of Health

If an accepted manuscript was funded by National Institutes of Health (NIH), the author may inform editors of the NIH funding number. The editors are able to deposit the paper to the NIH Manuscript Submission System on behalf of the author.

2. Submission Preparation

2.1 Cover Letter

A cover letter is required to be submitted accompanying each manuscript. Here is a guideline of a cover letter for authors’ consideration:

List the highlights of the current manuscript and no more than 5 short sentences;

All authors have read the final manuscript, have approved the submission to the journal, and have accepted full responsibilities pertaining to the manuscript’s delivery and contents;

Clearly state that the manuscript is an original work on its own merit, that it has not been previously published in whole or in part, and that it is not being considered for publication elsewhere;

No materials are reproduced from another source (if there is material in your manuscript that has been reproduced from another source, please state whether you have obtained permission from the copyright holder to use them);

Conflicts of interest statement;

If the manuscript is contributed to a Special Issue, please also mention it in the cover letter;

If the manuscript was presented partly or entirely in a conference, the author should clearly state the background information of the event, including the conference name, time, and place in the cover letter.

2.2 Types of Manuscripts

There is no restriction on the length of manuscripts, number of figures, tables and references, provided that the manuscript is concise and comprehensive. The journal publishes Research Article, Review, Technical Note, *etc*. For more details about paper type, please refer to the following table.

Manuscript Type	Definition	Word Limit	Abstract	Keywords	Main Text Structure
Research Article	A Research Article is a seminal and insightful research study and showcases that often involves modern techniques or methodologies. Authors should justify that their work is of novel findings	8000 max	The abstract should state briefly the purpose of the research, the principal results and major conclusions. No more than 250 words	3-8 keywords	The main content should include four sections: Introduction, Methods, Results and Discussion
Review	A Review should be an authoritative, well balanced, and critical survey of recent progress in an attractive or a fundamental research field	10000 max	Unstructured abstract. No more than 250 words	3-8 keywords	The main text may consist of several sections with unfixed section titles. We suggest that the author include an "Introduction" section at the beginning, several sections with unfixed titles in the middle part, and a "Conclusions" section at the end
Technical Note	A Technical Note is a short article giving a brief description of a specific development, technique, or procedure, or it may describe a modification of an existing technique, procedure or device applied in research	3500 max	Unstructured abstract. No more than 250 words	3-8 keywords	/
Editorial	An Editorial is a short article describing news about the journal or opinions of senior Editors or the publisher	1000 max	None required	None required	/
Commentary	A Commentary is to provide comments on a newly published article or an alternative viewpoint on a certain topic	2500 max	Unstructured abstract. No more than 250 words	3-8 keywords	/
Perspective	A Perspective provides personal points of view on the state-of-the-art of a specific area of knowledge and its future prospects	2000 max	Unstructured abstract. No more than 250 words	3-8 keywords	/

2.3 Manuscript Structure

2.3.1 Front Matter

2.3.1.1 Title

The title of the manuscript should be concise, specific and relevant, with no more than 16 words if possible.

2.3.1.2 Authors and Affiliations

Authors' full names should be listed. The initials of middle names can be provided. The affiliations and email addresses for all authors should be listed. At least one author should be designated as the corresponding author. In addition, corresponding authors are suggested to provide their Open Researcher and Contributor ID upon submission. Please note that any change to authorship is not allowed after manuscript acceptance. The authors' affiliations should be provided in this format: department, institution, city, postcode, country.

2.3.1.3 Abstract
The abstract should be a single paragraph with word limitation and specific structure requirements (for more details please refer to Types of Manuscripts). It usually describes the main objective(s) of the study, explains how the study was done, including any model organisms used, without methodological detail, and summarizes the most important results and their significance. The abstract must be an objective representation of the study: it is not allowed to contain results that are not presented and substantiated in the manuscript, or exaggerate the main conclusions. Citations should not be included in the abstract.

2.3.1.4 Graphical Abstract
The graphical abstract is essential as this can catch first view of your publication by readers. We recommend you submit an eye-catching figure. It should summarize the content of the article in a concise graphical form. It is recommended to use it because this can make online articles get more attention.

The graphical abstract should be submitted as a separate document in the online submission system. Please provide an image with a minimum of 531 × 1,328 pixels (h × w) or proportionally more. The image should be readable at a size of 5 cm × 13 cm using a regular screen resolution of 96 dpi. Preferred file types: TIFF, PSD, AI, JPEG, and EPS files.

2.3.1.5 Keywords
Three to eight keywords should be provided, which are specific to the article, yet reasonably common within the subject discipline.

Sections 2.3.1.1 and 2.3.1.2 should appear in all manuscript types.

2.3.2 Main Text
Manuscripts of different types are structured with different sections of content. Please refer to Types of Manuscripts to make sure which sections should be included in the manuscripts.

2.3.2.1 Introduction
The introduction should contain background that puts the manuscript into context, allow readers to understand why the study is important, include a brief review of key literature, and conclude with a brief statement of the overall aim of the work and a comment about whether that aim was achieved. Relevant controversies or disagreements in the field should be introduced as well.

2.3.2.2 Methods
The methods should contain sufficient details to allow others to fully replicate the study. New methods and protocols should be described in detail while well-established methods can be briefly described or appropriately cited. Statistical terms, abbreviations, and all symbols used should be defined clearly. Protocol documents for clinical trials, observational studies, and other non-laboratory investigations may be uploaded as supplementary materials.

2.3.2.3 Results
This section contains the findings of the study. Results of statistical analysis should also be included either as text or as tables or figures if appropriate. Authors should emphasize and summarize only the most important observations. Data on all primary and secondary outcomes identified in the section Methods should also be provided. Extra or supplementary materials and technical details can be placed in supplementary documents.

2.3.2.4 Discussion
This section should discuss the implications of the findings in context of existing research and highlight limitations of the study. Future research directions may also be mentioned.

2.3.2.5 Conclusion
It should state clearly the main conclusions and include the explanation of their relevance or importance to the field.

2.3.3 Back Matter
The following sections should appear in all manuscript types.

2.3.3.1 Acknowledgments
Anyone who contributed towards the article but does not meet the criteria for authorship, including those who provided professional writing services or materials, should be acknowledged. Authors should obtain permission to acknowledge from all those mentioned in the Acknowledgments section. This section is not added if the author does not have anyone to acknowledge.

2.3.3.2 Authors' Contributions

Each author is expected to have made substantial contributions to the conception or design of the work, or the acquisition, analysis, or interpretation of data, or the creation of new software used in the work, or have drafted the work or substantively revised it.

Please use Surname and Initial of Forename to refer to an author's contribution. For example: made substantial contributions to conception and design of the study and performed data analysis and interpretation: Salas H, Castaneda WV; performed data acquisition, as well as providing administrative, technical, and material support: Castillo N, Young V.

If an article is single-authored, please include "The author contributed solely to the article." in this section.

2.3.3.3 Availability of Data and Materials

In order to maintain the integrity, transparency and reproducibility of research records, authors should include this section in their manuscripts, detailing where the data supporting their findings can be found. Data can be deposited into data repositories or published as supplementary information in the journal. Authors who cannot share their data should state that the data will not be shared and explain it. If a manuscript does not involve such issues, please state "Not applicable." in this section.

2.3.3.4 Financial Support and Sponsorship

All sources of funding for the study reported should be declared. The role of the funding body in the experiment design, collection, analysis and interpretation of data, and writing of the manuscript should be declared. Any relevant grant numbers and the link of funder's website should be provided if any. If the study is not involved with this issue, state "None." in this section.

2.3.3.5 Conflicts of Interest

Authors must declare any potential conflicts of interest that may be perceived as inappropriately influencing the representation or interpretation of reported research results. If there are no conflicts of interest, please state "All authors declared that there are no conflicts of interest." in this section. Some authors may be bound by confidentiality agreements. In such cases, in place of itemized disclosures, we will require authors to state "All authors declared that they are bound by confidentiality agreements that prevent them from disclosing their conflicts of interest in this work.". If authors are unsure whether conflicts of interest exist, please refer to the "Conflicts of Interest" of *Complex Engineering Systems* (*CES*) Editorial Policies for a full explanation.

2.3.3.6 Ethical Approval and Consent to Participate

Research involving human subjects, human material or human data must be performed in accordance with the Declaration of Helsinki and approved by an appropriate ethics committee. An informed consent to participate in the study should also be obtained from participants, or their parents or legal guardians for children under 16. A statement detailing the name of the ethics committee (including the reference number where appropriate) and the informed consent obtained must appear in the manuscripts reporting such research.

Studies involving animals and cell lines must include a statement on ethical approval. More information is available at Editorial Policies.

If the manuscript does not involve such issues, please state "Not applicable." in this section.

2.3.3.7 Consent for Publication

Manuscripts containing individual details, images or videos, must obtain consent for publication from that person, or in the case of children, their parents or legal guardians. If the person has died, consent for publication must be obtained from the next of kin of the participant. Manuscripts must include a statement that written informed consent for publication was obtained. Authors do not have to submit such content accompanying the manuscript. However, these documents must be available if requested. If the manuscript does not involve this issue, state "Not applicable." in this section.

2.3.3.8 Copyright

Authors retain copyright of their works through a Creative Commons Attribution 4.0 International License that clearly states how readers can copy, distribute, and use their attributed research, free of charge. A declaration "© The Author(s) 2023." will be added to each article. Authors are required to sign a License to Publish before formal publication.

2.3.3.9 References

References should be numbered in order of appearance at the end of manuscripts. In the text, reference numbers should be placed in square brackets and the corresponding references are cited thereafter. List all authors when the number of authors

is less than or equal to six, if there are more than six authors, only the first three authors' names should be listed, other authors' names should be omitted and replaced with "et al.". The journal's name should be required to be italicized and the journal references should have corresponding DOI numbers. Information from manuscripts accepted but not published should be cited in the text as "Unpublished material" with written permission from the source. Journal names should be abbreviated according to the List of Title Word Abbreviations.

References should be described as follows, depending on the types of works:

Types	**Examples**
Journal articles by individual authors	Cao MS, Pan LX, Gao YF, et al. Neural network ensemble-based parameter sensitivity analysis in civil engineering systems. *Neural Comput Applic* 2017;28:1583-90. [DOI: 10.1007/s00521-015-2132-4]
Organization as author	Diabetes Prevention Program Research Group. Hypertension, insulin, and proinsulin in participants with impaired glucose tolerance. *Hypertension* 2002;40:679-86. [DOI: 10.1161/01.hyp.0000035706.28494.09]
Both personal authors and organization as author	Vallancien G, Emberton M, Harving N, van Moorselaar RJ; Alf-One Study Group. Sexual dysfunction in 1,274 European men suffering from lower urinary tract symptoms. *J Urol* 2003;169:2257-61. [DOI: 10.1097/01.ju.0000067940.76090.73]
Journal articles not in English	Mao X, Ding YK. Sentiment feature analysis and harmonic sense evaluation of images. *J Electronic* 2001;29:23-7. (in Chinese)
Journal articles ahead of print	Albasir A, Hu Q, Naik K, Naik N. Unsupervised detection of security threats in cyberphysical system and IoT devices based on power fingerprints and RBM autoencoders. *J Surveill Secur Saf* 2021; Epub ahead of print [DOI: 10.20517/jsss.2020.19]
Books	Gaydon AG, Wolfhard HG. Flames. 2nd ed. London: Chapman and Hall Ltd.; 1960. pp. 10-20.
Book chapters	Chothia T, Smirnov V. A traceability attack against e-passports. In: Sion R, Editor. Financial cryptography. Lecture notes in computer science. Springer; 2010. pp. 20-34..
Online resource	Intel Technology Journal. Developing smart toys - from idea to product. Available from: https://www.intel.com/content/dam/www/public/us/en/documents/research/2001-vol05-iss-4-intel-technology-journal.pdf. [Last accessed on 20 Feb 2021]
Conference proceedings	Harnden P, Joffe JK, Jones WG, Editors. Germ cell tumours V. Proceedings of the 5th Germ Cell Tumour Conference; 2001 Sep 13-15; Leeds, UK. New York: Springer; 2002..
Conference paper	Christensen S, Oppacher F. An analysis of Koza's computational effort statistic for genetic programming. In: Foster JA, Lutton E, Miller J, Ryan C, Tettamanzi AG, Editors. Genetic programming. EuroGP 2002: Proceedings of the 5th European Conference on Genetic Programming; 2002 Apr 3-5; Kinsdale, Ireland. Berlin: Springer; 2002. pp. 182-91.
Unpublished material	Tian D, Araki H, Stahl E, Bergelson J, Kreitman M. Signature of balancing selection in Arabidopsis. Proc Natl Acad Sci U S A. Forthcoming 2002.

The journal also recommends that authors prepare references with a bibliography software package, such as EndNote to avoid typing mistakes and duplicated references.

2.3.3.10 Supplementary Materials

Additional data and information can be uploaded as Supplementary Materials to accompany the manuscripts. The supplementary materials will also be available to the referees as part of the peer-review process. Any file format is acceptable, such as data sheet (word, excel, csv, cdx, fasta, pdf or zip files), presentation (powerpoint, pdf or zip files), image (cdx, eps, jpeg, pdf, png or tiff), table (word, excel, csv or pdf), audio (mp3, wav or wma) or video (avi, divx, flv, mov, mp4, mpeg, mpg or wmv). All information should be clearly presented. Supplementary materials should be cited in the main text in numeric order (e.g., Supplementary Figure 1, Supplementary Figure 2, Supplementary Table 1, Supplementary Table 2, *etc*.). The style of supplementary figures or tables complies with the same requirements on figures or tables in main text. Videos and audios should be prepared in English, and limited to a size of 500 MB.

2.4 Manuscript Format

2.4.1 File Format

Manuscript files can be in DOC and DOCX formats and should not be locked or protected.

Manuscript prepared in LaTex must be collated into one ZIP folder (including all source files and images, so that the Editorial Office can recompile the submitted PDF).

When preparing manuscripts in different file formats, please use the corresponding Manuscript Templates.

2.4.2 Length

There are no restrictions on paper length, number of figures, or number of supporting documents. Authors are encouraged

to present and discuss their findings concisely.

2.4.3 Language

Manuscripts must be written in English.

2.4.4 Multimedia Files

The journal supports manuscripts with multimedia files. The requirements are listed as follows:

Video or audio files are only acceptable in English. The presentation and introduction should be easy to understand. The frames should be clear, and the speech speed should be moderate;
A brief overview of the video or audio files should be given in the manuscript text;
The video or audio files should be limited to a size of up to 500 MB;
Please use professional software to produce high-quality video files, to facilitate acceptance and publication along with the submitted article. Upload the videos in mp4, wmv, or rm format (preferably mp4) and audio files in mp3 or wav format.

2.4.5 Figures

Figures should be cited in numeric order (e.g., Figure 1, Figure 2) and placed after the paragraph where it is first cited;

Figures can be submitted in format of TIFF, PSD, AI, EPS or JPEG, with resolution of 300-600 dpi;

Figure caption is placed under the Figure;

Diagrams with describing words (including, flow chart, coordinate diagram, bar chart, line chart, and scatter diagram, *etc.*) should be editable in word, excel or powerpoint format. Non-English information should be avoided;

Labels, numbers, letters, arrows, and symbols in figure should be clear, of uniform size, and contrast with the background;

Symbols, arrows, numbers, or letters used to identify parts of the illustrations must be identified and explained in the legend;

Internal scale (magnification) should be explained and the staining method in photomicrographs should be identified;

All non-standard abbreviations should be explained in the legend;

Permission for use of copyrighted materials from other sources, including re-published, adapted, modified, or partial figures and images from the internet, must be obtained. It is authors' responsibility to acquire the licenses, to follow any citation instruction requested by third-party rights holders, and cover any supplementary charges.

2.4.6 Tables

Tables should be cited in numeric order and placed after the paragraph where it is first cited;

The table caption should be placed above the table and labeled sequentially (e.g., Table 1, Table 2);

Tables should be provided in editable form like DOC or DOCX format (picture is not allowed);

Abbreviations and symbols used in table should be explained in footnote;

Explanatory matter should also be placed in footnotes;

Permission for use of copyrighted materials from other sources, including re-published, adapted, modified, or partial tables from the internet, must be obtained. It is authors' responsibility to acquire the licenses, to follow any citation instruction requested by third-party rights holders, and cover any supplementary charges.

2.4.7 Abbreviations

Abbreviations should be defined upon first appearance in the abstract, main text, and in figure or table captions and used consistently thereafter. Non-standard abbreviations are not allowed unless they appear at least three times in the text. Commonly-used abbreviations, such as DNA, RNA, ATP, *etc.*, can be used directly without definition. Abbreviations in titles and keywords should be avoided, except for the ones which are widely used.

2.4.8 Italics

General italic words like vs., et al., etc., in vivo, in vitro; t test, F test, U test; related coefficient as r, sample number as n, and probability as P; names of genes; names of bacteria and biology species in Latin.

2.4.9 Units

SI Units should be used. Imperial, US customary and other units should be converted to SI units whenever possible. There is a space between the number and the unit (i.e., 23 mL). Hour, minute, second should be written as h, min, s.

2.4.10 Numbers

Numbers appearing at the beginning of sentences should be expressed in English. When there are two or more numbers in a paragraph, they should be expressed as Arabic numerals; when there is only one number in a paragraph, number < 10 should be expressed in English and number > 10 should be expressed as Arabic numerals. 12345678 should be written as 12,345,678.

2.4.11 Equations

Equations should be editable and not appear in a picture format. Authors are advised to use either the Microsoft Equation Editor or the MathType for display and inline equations.

Display equations should be numbered consecutively, using Arabic numbers in parentheses;
Inline equations should not be numbered, with the same/similar size font used for the main text.

2.4.12 Headings

In the main body of the paper, three different levels of headings may be used.

Level one headings: they should be in bold, and numbered using Arabic numbers, such as 1. INTRODUCTION, and 2. METHODS, with all letters capitalized;
Level two headings: they should be in bold and numbered after the level one heading, such as 2.1 Statistical analyses, 2.2 ..., 2.3..., *etc*., with the first letter capitalized;
Level three headings: they should be italicized, and numbered after the level two heading, such as 2.1.1 Data distributions,and 2.1.2 outliers and linear regression, with the first letter capitalized.

2.4.13 Text Layout

As the electronic submission will provide the basic material for typesetting, it is important to prepare papers in the general editorial style of the journal.

The font is Times New Roman;
The font size is 12pt;
Single column, 1.5x line spacing;
Insert one line break (one Return) before the heading and paragraph, if the heading and paragraph are adjacent, insert a line break before the heading only;
No special indentation;
Alignment is left end;
Insert consecutive line numbers;
For other details please refer to the Manuscript Templates.

2.5 Submission Link

Submit an article via https://oaemesas.com/login?JournalId=comengsys.

3. Research and Publication Ethics

3.1 Research Involving Human Subjects

All studies involving human subjects must be in accordance with the Helsinki Declaration and seek approval to conduct the study from an independent local, regional, or national review body (e.g., ethics committee, institutional review board, *etc*.). Such approval, including the names of the ethics committee, institutional review board, *etc*., must be listed in a declaration statement of Ethical Approval and Consent to Participate in the manuscript. If the study is judged exempt from ethics approval, related information (e.g., name of the ethics committee granting the exemption and the reason for the exemption) must be listed. Further documentation on ethics should also be prepared, as Editors may request more detailed information. Manuscripts with suspected ethical problems will be investigated according to COPE Guidelines.

3.1.1 Consent to Participate

For all studies involving human subjects, informed consent to participate in the studies must be obtained from participants, or their parents or legal guardians for children under 16. Statements regarding consent to participate should be included in a declaration statement of Ethical Approval and Consent to Participate in the manuscript. If informed consent is not required, the name of the ethics committee granting the exemption and the reason for the exemption must be listed. If any ethical violation is found at any stage of publication, the issue will be investigated seriously based on COPE Guidelines.

3.1.2 Consent for Publication

All articles published by OAE are freely available on the Internet. All manuscripts that include individual participants' data in any form (i.e., details, images, videos, *etc.*) will not be published without Consent for Publication obtained from that person(s), or for children, their parents, or legal guardians. If the person has died, Consent for Publication must be obtained from the next of kin. Authors must add a declaration statement of Consent for Publication in the manuscript, specifying written informed consent for publication has been obtained.

3.1.3 Trial Registration

OAE requires all authors to register all relevant clinical trials that are reported in manuscripts submitted. OAE follows the World Health Organization (WHO)'s definition of clinical trials: "A clinical trial is any research study that prospectively assigns human participants or groups of humans to one or more health-related interventions to evaluate the effects on health outcomes. Interventions include but are not restricted to drugs, cells, other biological products, surgical procedures, radiologic procedures, devices, behavioral treatments, process-of-care changes, preventive care, *etc.*".

In line with International Committee of Medical Journal Editors (ICMJE) Recommendations, OAE requires the registration of clinical trials in a public trial registry at or before the time of first patient enrollment. OAE accepts publicly accessible registration in any registry that is a primary register of the WHO International Clinical Trials Registry Platform or in ClinicalTrials.gov. The trial registration number should be listed at the end of the Abstract section.

Secondary data analyses of primary (parent) clinical trials should not be registered as a new clinical trial, but rather reference the trial registration number of the primary trial.

Editors of OAE journals will consider carefully whether studies failed to register or had an incomplete trial registration. Because of the importance of prospective trial registration, if there is an exception to this policy, trials must be registered and the authors should indicate in the publication when registration was completed and why it was delayed. Editors will publish a statement indicating why an exception was allowed. Please note such exceptions should be rare, and authors failing to prospectively register a trial risk its inadmissibility to OAE journals.

Authors who are not sure whether they need trial registration may refer to ICMJE FAQs for further information.

3.2 Research Involving Animals

Experimental research on animals should be approved by an appropriate ethics committee and must comply with institutional, national, or international guidelines. OAE encourages authors to comply with the AALAS Guidelines, the ARRIVE Guidelines, and/or the ICLAS Guidelines, and obtain prior approval from the relevant ethics committee. Manuscripts must include a statement indicating that the study has been approved by the relevant ethical committee and the whole research process complies with ethical guidelines. If a study is granted an exemption from requiring ethics approval, the name of the ethics committee granting the exemption and the reason(s) for the exemption should be detailed. Editors will take account of animal welfare issues and reserve the right to reject a manuscript, especially if the research involves protocols that are inconsistent with commonly accepted norms of animal research.

3.3 Research Involving Cell Lines

Authors must describe what cell lines are used and their origin so that the research can be reproduced. For established cell lines, the provenance should be stated and references must also be given to either a published paper or to a commercial source. For de novo cell lines derived from human tissue, appropriate approval from an institutional review board or equivalent ethical committee, and consent from the donor or next of kin, should be obtained. Such statements should be listed on the Declaration section of Ethical Approval and Consent to Participate in the manuscript.

Further information is available from the International Cell Line Authentication Committee (ICLAC). OAE recommends that authors check the NCBI database for misidentification and contamination of human cell lines.

3.4 Research Involving Plants

Experimental research on plants (either cultivated or wild), including collection of plant material, must comply with institutional, national, or international guidelines. Field studies should be conducted in accordance with local legislation, and the manuscript should include a statement specifying the appropriate permissions and/or licenses. OAE recommends that authors comply with the IUCN Policy Statement on Research Involving Species at Risk of Extinction and the Convention on the Trade in Endangered Species of Wild Fauna and Flora.

For each submitted manuscript, supporting genetic information and origin must be provided for plants that were utilized. For research manuscripts involving rare and non-model plants (other than, e.g., Arabidopsis thaliana, Nicotiana benthamiana, Oriza sativa, or many other typical model plants), voucher specimens must be deposited in a public herbarium or other public collections providing access to deposited materials.

3.5 Publication Ethics Statement

OAE is a member of the Committee on Publication Ethics (COPE). We fully adhere to its Code of Conduct and to its Best Practice Guidelines.

The Editors of this journal enforce a rigorous peer-review process together with strict ethical policies and standards to guarantee to add high-quality scientific works to the field of scholarly publication. Unfortunately, cases of plagiarism, data falsification, image manipulation, inappropriate authorship credit, and the like, do arise. The Editors of *CES* take such publishing ethics issues very seriously and are trained to proceed in such cases with zero tolerance policy.

Authors wishing to publish their papers in *CES* must abide by the following:

The author(s) must disclose any possibility of a conflict of interest in the paper prior to submission;
The authors should declare that there is no academic misconduct in their manuscript in the cover letter;
Authors should accurately present their research findings and include an objective discussion of the significance of their findings;
Data and methods used in the research need to be presented in sufficient detail in the manuscript so that other researchers can replicate the work;
Authors should provide raw data if referees and the Editors of the journal request;
Simultaneous submission of manuscripts to more than one journal is not tolerated;
Republishing content that is not novel is not tolerated (for example, an English translation of a paper that is already published in another language will not be accepted);
The manuscript should not contain any information that has already been published. If you include already published figures or images, please get the necessary permission from the copyright holder to publish under the CC-BY license;
Plagiarism, data fabrication and image manipulation are not tolerated;
Plagiarism is not acceptable in OAE journals.

Plagiarism involves the inclusion of large sections of unaltered or minimally altered text from an existing source without appropriate and unambiguous attribution, and/or an attempt to misattribute original authorship regarding ideas or results, and copying text, images, or data from another source, even from your own publications, without giving credit to the source. As to reusing the text that is copied from another source, it must be between quotation marks and the source must be cited. If a study's design or the manuscript's structure or language has been inspired by previous studies, these studies must be cited explicitly.

If plagiarism is detected during the peer-review process, the manuscript may be rejected. If plagiarism is detected after publication, we may publish a Correction or retract the paper.

Falsification is manipulating research materials, equipment, or processes, or changing or omitting data or results so that the findings are not accurately represented in the research record.

Image files must not be manipulated or adjusted in any way that could lead to misinterpretation of the information provided by the original image.

Irregular manipulation includes: introduction, enhancement, moving, or removing features from the original image; grouping of images that should be presented separately, or modifying the contrast, brightness, or color balance to obscure, eliminate, or enhance some information.

If irregular image manipulation is identified and confirmed during the peer-review process, we may reject the manuscript. If irregular image manipulation is identified and confirmed after publication, we may publish a Correction or retract the paper.

OAE reserves the right to contact the authors' institution(s) to investigate possible publication misconduct if the Editors find conclusive evidence of misconduct before or after publication. OAE has a partnership with iThenticate, which is the most trusted similarity checker. It is used to analyze received manuscripts to avoid plagiarism to the greatest extent possible. When plagiarism becomes evident after publication, we will retract the original publication or require modifications, depending on the degree of plagiarism, context within the published article, and its impact on the overall integrity of the published study. Journal Editors will act under the relevant COPE guidelines.

4. Authorship

Authorship credit of *CES* should be solely based on substantial contributions to a published study, as specified in the

following four criteria:

1. Substantial contributions to the conception or design of the work, or the acquisition, analysis, or interpretation of data for the work;
2. Drafting the work or revising it critically for important intellectual content;
3. Final approval of the version to be published;
4. Agreement to be accountable for all aspects of the work in ensuring that questions related to the accuracy or integrity of any part of the work are appropriately investigated and resolved.

All those who meet these criteria should be identified as authors. Authors must specify their contributions in the section Authors'' Contributions of their manuscripts. Contributors who do not meet all the four criteria (like only involved in acquisition of funding, general supervision of a research group, general administrative support, writing assistance, technical editing, language editing, proofreading, *etc*.) should be acknowledged in the section of Acknowledgement in the manuscript rather than being listed as authors.

If a large multiple-author group has conducted the work, the group ideally should decide who will be authors before the work starts and confirm authors before submission. All authors of the group named as authors must meet all the four criteria for authorship.

AI and AI-assisted technologies should not be listed as an author or co-author.

5. Reviewers Exclusions

You are welcome to exclude a limited number of researchers as potential Editors or reviewers of your manuscript. To ensure a fair and rigorous peer review process, we ask that you keep your exclusions to a maximum of three people. If you wish to exclude additional referees, please explain or justify your concerns—this information will be helpful for Editors when deciding whether to honor your request.

6. Editors and Journal Staff as Authors

Editorial independence is extremely important and OAE does not interfere with Editorial decisions. Editorial staff or Editors shall not be involved in processing their own academic work. Submissions authored by Editorial staff/Editors will be assigned to at least three independent outside reviewers. Decisions will be made by the Editor-in-Chief, including Special Issue papers. Journal staff are not involved in the processing of their own work submitted to any OAE journals.

7. Policy of the Use of AI and AI-assisted Technologies in Scientific Writing

Generative AI and AI-assisted technologies (e.g., large language models) are expected to be increasingly used to create content. In the writing process of manuscripts, using AI and AI-assisted technologies to complete key researcher work, such as producing scientific insights, analyzing and interpreting data or drawing scientific conclusions, is not allowed, and they should only be used to improve the readability and language of manuscripts.

AI and AI-assisted technologies should be used under human control and supervision as they may generate incorrect or prejudiced output, and they should not be listed as an author or co-author, nor cited as an author.

The use of AI and AI-assisted technologies should be disclosed by authors in their manuscripts, and a statement will be required in the final publication.

OAE will keep monitoring the development and adjust the policy when necessary.

8. Conflict of Interests

OAE journals require authors to declare any possible financial and/or non-financial conflicts of interest at the end of their manuscript and in the cover letter, as well as confirm this point when submitting their manuscript in the submission system. If no conflicts of interest exist, authors need to state "All authors declared that there are no conflicts of interest". We also recognize that some authors may be bound by confidentiality agreements, in which cases authors need to state "All authors declared that they are bound by confidentiality agreements that prevent them from disclosing their competing interests in this work".OAE will keep monitoring the development and adjust the policy when necessary.

9. Editorial Process

9.1 Pre-Check

New submissions are initially checked by the Managing Editor from the perspectives of originality, suitability, structure and formatting, conflicts of interest, background of authors, *etc*. Poorly prepared manuscripts may be rejected at this stage. If your manuscript does not meet one or more of these requirements, we will return it for further revisions.

Once your manuscript has passed the initial check, it will be assigned to the Assistant Editor, and then the Editor-in-Chief, or an Associate Editor in the case of a conflict of interest, will be notified of the submission and invited to review. Regarding Special Issue paper, after passing the initial check, the manuscript will be successively assigned to the Assistant Editor, and then to the Editor-in-Chief, or an Associate Editor in the case of conflict of interest for the Editor-in-Chief to review. The Editor-in-Chief, or the Associate Editor may reject manuscripts that they deem highly unlikely to pass peer review without further consultation. Once your manuscript has passed the Editorial assessment, the Associate Editor will start to organize peer-review.

All manuscripts submitted to *CES* are screened using CrossCheck powered by iThenticate to identify any plagiarized content. Your study must also meet all ethical requirements as outlined in our Editorial Policies. If the manuscript does not pass any of these checks, we may return it to you for further revisions or decline to consider your study for publication.

9.2 Peer Review

CES operates a single-blind review process, which means that reviewers know the names of authors, but the names of the reviewers are hidden from the authors. The scientific quality of the research described in the manuscript is assessed by a minimum of three independent expert reviewers. The Editor-in-Chief is responsible for the final decision regarding acceptance or rejection of the manuscript.

All information contained in your manuscript and acquired during the review process will be held in the strictest confidence.

9.3 Decisions

Your research will be judged on scientific soundness only, not on its perceived impact as judged by Editors or referees. There are three possible decisions: Accept (your study satisfies all publication criteria), Invitation to Revise (more work is required to satisfy all criteria), and Reject (your study fails to satisfy key criteria and it is highly unlikely that further work can address its shortcomings). All of the following publication criteria must be fulfilled to enable your manuscript to be accepted for publication:

Originality

The study reports original research and conclusions.

Data availability

All data to support the conclusions either have been provided or are otherwise publicly available.

Statistics

All data have been analyzed through appropriate statistical tests and these are clearly defined.

Methods

The methods are described in sufficient detail to be replicated.

Citations

Previous work has been appropriately acknowledged.

Interpretation

The conclusions are a reasonable extension of the results.

Ethics

The study design, data presentation, and writing style comply with our Editorial Policies.

9.4 Revisions

Authors are required to submit the revised manuscript within one week if minor revision is recommended while two weeks if major revision recommended or one month if additional experiments are needed. If authors need more than one month to revise their manuscript, we usually require the authors to resubmit their paper. We request that a document of point-to-point response to all comments of reviewers and the Editor-in-Chief or the Associate Editor should be supplied along with the revised manuscript to allow quick assessment of your revised manuscript. This document should outline in detail how each of the comments was addressed in the revised manuscript or should provide a rebuttal to the criticism. Manuscripts may or may not be sent to reviewers after revision, dependent on whether the reviewer requested to see the revised version. Apart from in exceptional circumstances, *CES* only supports a round of major revision per manuscript.

10. Contact Us

Journal Contact
Complex Engineering Systems Editorial Office
Suite 1504, Tower A, Xi'an National Digital Publishing Base, No. 996 Tiangu 7th Road, Gaoxin District, Xi'an 710077, Shaanxi, China.

Wen Zhang
Managing Editor
editorial@comengsys.com

Last updated on 2 June, 2023

www.oaepublish.com

Complex Engineering Systems
(*CES*)
Los Angeles Office
245 E Main Street Ste 107, Alhambra,
CA 91801, USA
E-mail: editorial@comengsys.com
Website: www.comengsys.com.